Research and Experimental Testing on Structural Elements and Systems Using THERMASTEEL Panels

contract no. 31160/04.09.2024

REPORT

Experimental Testing of Two Structures Assembled on the Seismic Platform

- Structure 1 – Model THS 24-388 (steel 0.84 mm, EPS 24kg/m^3)
- Structure 2 – Model THS 24-389 (steel 1.09mm, EPS 16.9kg/m^3)

Beneficiary:	SC ABC CONSTRUCTII CIVILE SI INDUSTRIALE SRL, Bucharest, Romania Administrator: **Eng. Amedeo Stoian**
Contract director nr. 31160/04.09.2024:	"Gheorghe Asachi" Technical University of Iasi, Romania **Lecturer, PhD Eng. George ȚĂRANU**
Partner:	ICECON SA, Bucharest, Romania **PhD. Eng. Cristina SESCU-GAL**

05 March 2026

Research Team within the Research Contract

Nr. crt.	Full name	Role within the Project/Contract	Academic or Research Position
1	George ȚĂRANU	Contract Director	Șef lucrări dr. Ing. TUIASI
2	Mihai BUDESCU	Project Team Member	Professor Emeritus, TUIASI
3	Vasile-Mircea VENGHIAC	Project Team Member	Lecturer, PhD Eng., TUIASI
4	Mihai-Sergiu ALEXA-STRATULAT	Project Team Member	Physicist, PhD Eng., TUIASI
5	Rareș-George ȚĂRAN	Project Team Member	PhD Eng., TUIASI
6	Șerban IACOB	Project Team Member	PhD Student Eng., TUIASI

Table of contents

Figure list

1 INTRODUCTION

1.1 OBJECTIVE OF THE EXPERIMENTAL PROGRAM

The main objective of the experimental program is to evaluate the dynamic behavior of a structure made of prefabricated thermal-insulating panels of the *THERMASTEEL* type, subjected to controlled seismic actions applied through a high-precision testing platform.

The tests aim to characterize:

- the capacity of the structure to respond to bidirectional accelerograms (X and Y), with progressively increasing values of peak acceleration;
- the response under resonance conditions, by applying a 5 Hz sinusoidal beat excitation;
- the global and local deformability of both the panels and the assembled structural system;
- the influence of direction and intensity of the input signal on the response at the top, compared to the base of the structure.

In addition, the program aims to validate the accuracy of the measurement methods used (wireless accelerometers and laser displacement transducers) and to obtain relevant data for future numerical model calibration.
All tests are conducted in accordance with the requirements of **Eurocode 8 (EN 1998-1)** and the Romanian seismic design code **P100**, concerning the behavior of structures under seismic actions.

The obtained results will contribute to understanding the performance of the *THERMASTEEL* structural system under seismic loading, providing a scientific basis for its application in seismic-prone areas and for validating the system within European Technical Assessment procedures.

1.2 REGULATORY AND TECHNICAL CONTEXT

The experimental program for testing the dynamic behavior of the structure made of *THERMASTEEL* prefabricated panels is carried out in the context of harmonizing European technical requirements for innovative lightweight construction systems.
Its purpose is to align with the provisions of **Eurocode 8 (EN 1998-1)** and **P100**, applicable to structural systems used in seismic regions.

Specifically, this program addresses the requirements from:

- **EN 1998-1:2004 (Eurocode 8)** – *Design of structures for earthquake resistance*, and
- **P100-1/2013** – *Seismic Design Code – Part I: Design Provisions for Buildings*,

which require the demonstration of resistance and stability capacity of the system under dynamic actions, including:

- the use of artificial or recorded accelerograms of sufficient duration (≥ 30 s);
- control of excitation levels through increasing values of **PGA (Peak Ground Acceleration)**;

- analysis of behavior through relative displacements and accelerations at key points;
- identification of natural frequencies;
- evaluation of the response in both transient and resonant regimes.

Regarding the measurement methodology and equipment, the tests comply with:

- the principles defined in **ISO 7626-2:2015 – Experimental Methods for Modal Analysis**, and
- best practices for the use of wireless accelerometers, LVDT transducers, and synchronized high-frequency data acquisition systems.

The tested structure represents a lightweight prefabricated composite system made of thin-walled steel frames and expanded polystyrene (EPS) core infill, manufactured by *THERMASTEEL*. It provides both structural and thermal-insulating functions and is currently undergoing technical validation for seismic performance.

Therefore, the data obtained within this program are essential for:

- characterization of actual seismic performance;
- defining usage limits based on seismic hazard level;
- supporting the technical documentation required to obtain technical approval.

This report thus constitutes a key technical document for the evaluation and certification stage under the current European regulations.

1.3 General Description of the Testing Method

The testing program was conducted using an ANCO R250-3123 seismic platform, capable of generating controlled movements in the horizontal plane along two directions (X and Y), as well as in the vertical direction (Z).

The purpose of the experimental method was to evaluate the dynamic response of a modular prefabricated structure made of THERMASTEEL panels, subjected to simulated seismic actions with progressively increasing intensity and varying spectral content.

The applied method consists of imposing input signals at the base of the structure (through the seismic platform) and recording the structural response at strategic points of the physical model.

A combination of wireless acceleration sensors and displacement transducers was used, enabling the simultaneous measurement of absolute motion in three directions and the calculation of relative displacements between the top and base of the structure — parameters that are essential for validating the structural performance.

2 TESTED STRUCTURAL MODELS. TYPE OF SYSTEM: SINGLE-STORY BUILDING CONSTRUCTED FROM THERMASTEEL PANELS

The two tested structural models, illustrated in Figures 1 and 2, are single-story modular buildings made entirely of prefabricated *THERMASTEEL* structural insulated panels. They were produced and delivered specifically for the seismic testing campaigns "Romania Seismic Test 1" and "Romania Seismic Test 2." Both models were assembled on the seismic platform using an adapter frame made of hot-rolled UPN 300 steel channels, as shown in Figure 3.

Fig. 1 – Structural model with THERMASTEEL panels – THS 24-388 (steel 0.84 mm, EPS 24 kg/m³), full-scale assembled

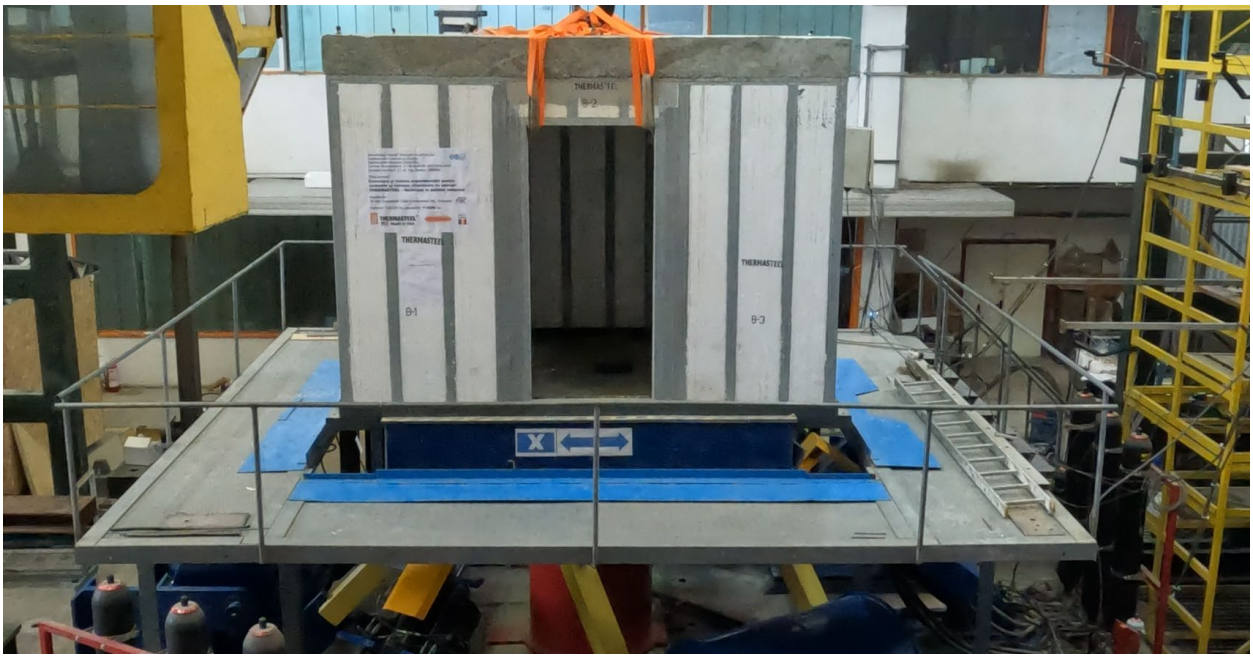

Fig. 2 – Structural model with THERMASTEEL panels – THS 24-389 (steel 1.09 mm, EPS 16.9 kg/m³)

2.1.1 Geometry and Composition

- **Total length**: 3632 mm
- **Total width**: 2794 mm
- **Total height**: 2705 mm
- **Types of panels used**: F -panel (for the floor slab) and W-panel (for exterior and load-bearing walls)
- **Panel thickness:** 7 ½ in (190 mm)
- **EPS core**:
  - 1.5 PCF (≈ 24 kg/m³) - THS 24-388
  - 1.0 PCF (≈ 16.9 kg/m³) THS 24-389
- **Steel Sheet thickness:**
  - THS 24-388 - 0.84 mm
  - THS 24-389 – 1.09 mm

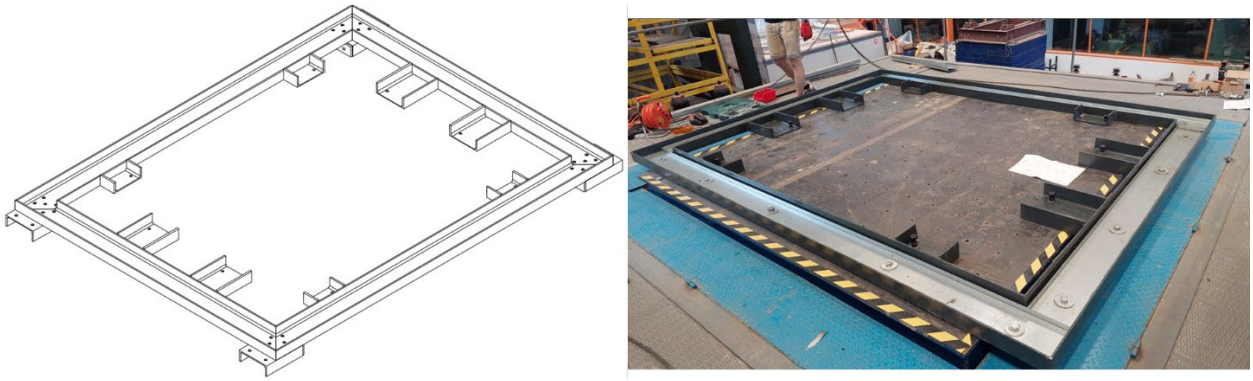

Fig. 3 – Adapter base frame made of UPN 300 channels and installation of the THERMASTEEL U-track (190 mm)

2.1.2 Construction Configuration

The panels include integrated light-gauge steel studs on both interior and exterior faces, arranged vertically and enclosed by a U-shaped 190 mm track (top and bottom track, 18 GA). Panel-to-panel connections are made through tongue-and-groove joints and steel tie plates (3 in × 5 in – 20 GA), fixed with #10-¾ in self-tapping screws spaced at 12 in (≈ 30 cm). Corner assemblies are completed using 24 GA L-profiles and header/sill plates for horizontal closures.

2.1.3 Construction Properties

The panels have an average specific weight of 15.4 kg/m², resulting in a low-mass structure typical of lightweight prefabricated systems. The closed-cell EPS core provides high thermal efficiency with a thermal resistance up to R-61, advantageous for energy-efficient applications.

Special *shear wall* panels were included, as defined in the design documentation, to resist lateral loads. The total weight of the reinforced concrete floor slab (deck + ribs + edge beams) is approximately 1.6 m³ × 2500 kg/m³ = 4000 kg.

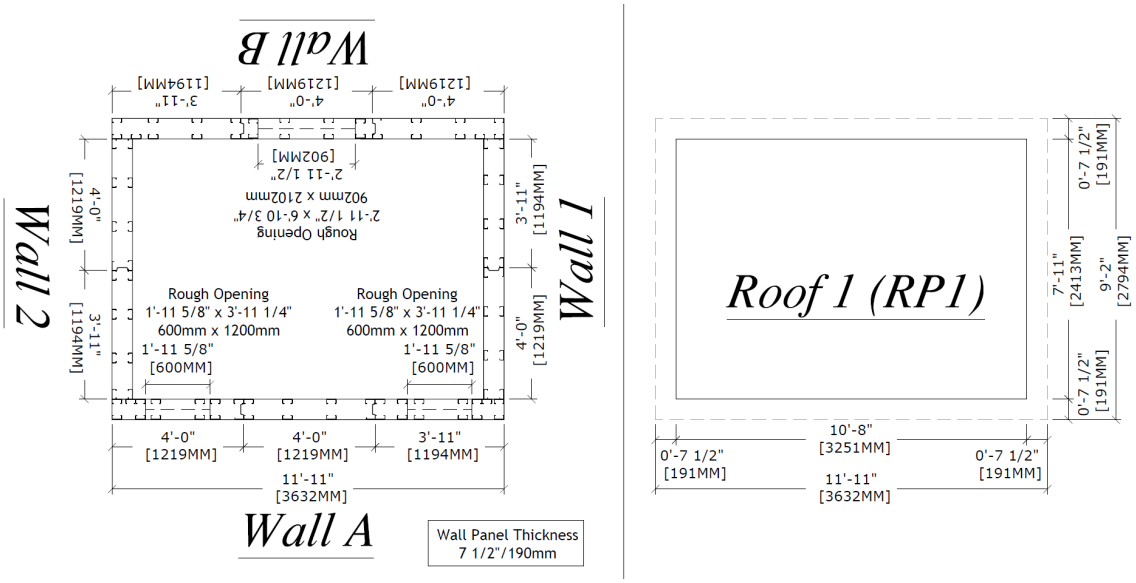

Fig. 4 – Assembly plan for wall-to-base and floor joints

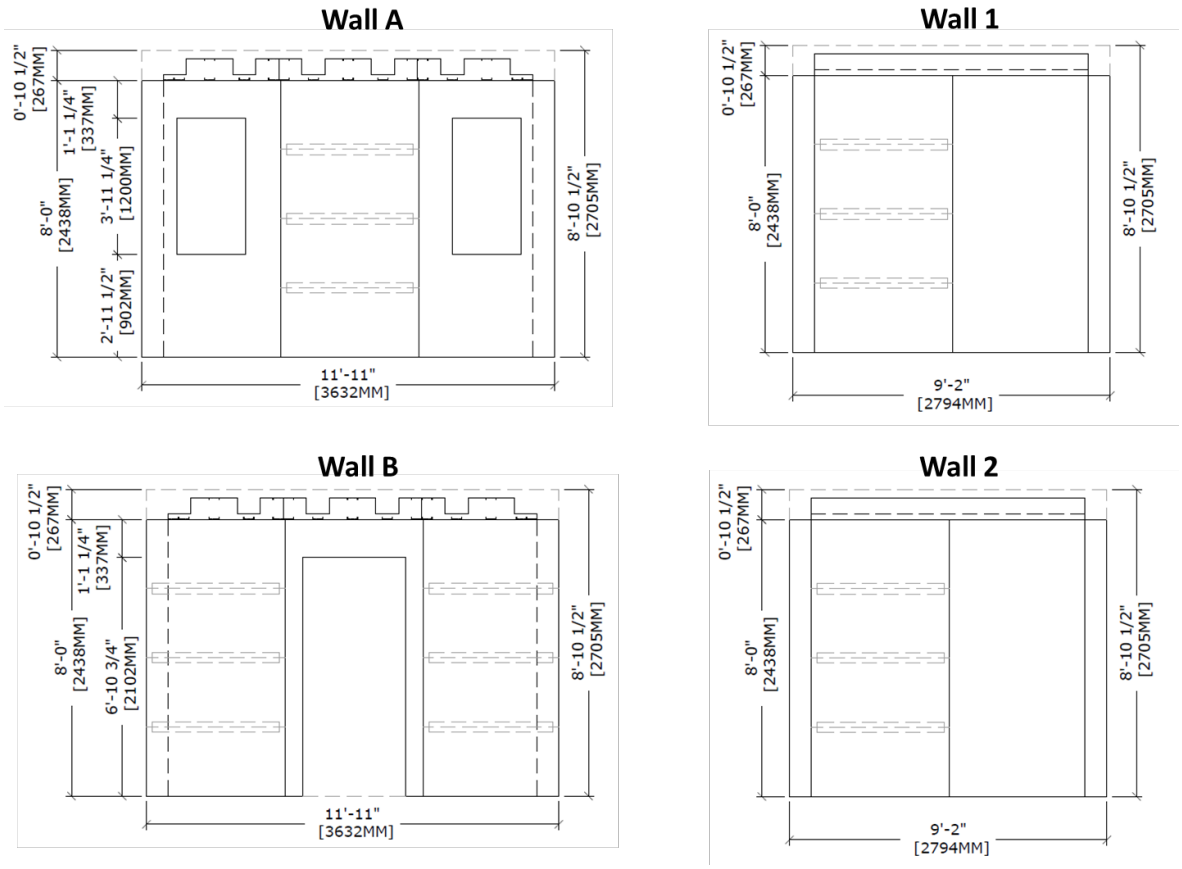

Fig. 5 – Assembly drawings for wall elevations

2.1.4 Panel Assembly and Casting of the Reinforced Concrete Slab

Figure 7 illustrates the stages of assembling the vertical and horizontal panels, as well as the placement of reinforcing bars for the floor slab. Reinforcement was made of B500C steel bars (Ø 8 mm and Ø 14 mm) bent with hooked ends. Concrete was mixed locally in a small batch mixer following a C30/37 class recipe; after seven days of curing, the achieved compressive strength and modulus of elasticity corresponded to a C16/20 class concrete. Three cylindrical specimens were cast and tested on the day of the seismic experiments (Figure 6). The measured elastic modulus was 25 000 MPa and the compressive strength 16 MPa.

2.1.5 Function and Purpose

The full-scale tested structure is representative of a single-story building system. The *THERMASTEEL* system, applicable to residential, commercial, and industrial constructions, is characterized by high energy efficiency and low weight. The experimental program aims to verify the structural behavior and resistance of such systems under dynamic and seismic actions in regions of moderate to high seismic hazard.

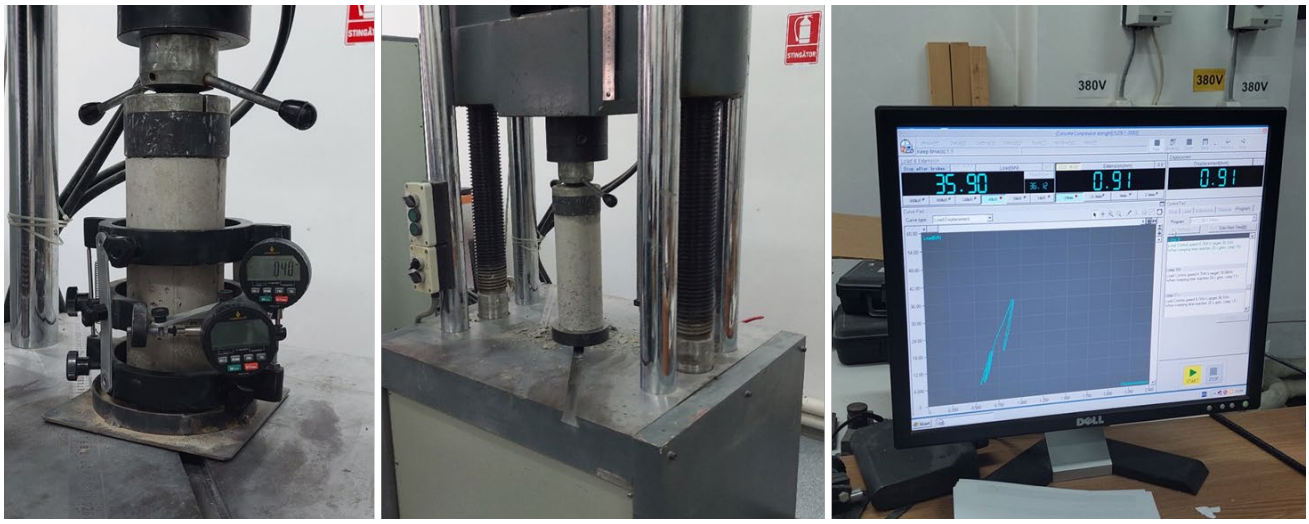

Fig. 6 – Testing of concrete cylinders to determine modulus of elasticity and compressive strength

Fig. 7 – Assembly of THERMASTEEL panels and structure erection

3 EQUIPMENT AND INSTRUMENTATION

3.1 SHAKING TABLE

To evaluate the seismic behavior of the structure made of *THERMASTEEL* panels, a seismic platform ANCO R250-3123, manufactured in 2004, was used. The equipment is installed in the testing hall of the Department of Structural Mechanics, Faculty of Civil Engineering and Building Services, *Gheorghe Asachi Technical University of Iasi*. The platform is capable of reproducing complex seismic motions. Its technical and operational characteristics are presented below:

1. **Degrees of Freedom and Motion Capacity**

The platform operates with three translational degrees of freedom, enabling motion along three orthogonal axes (X, Y, and Z). This configuration allows the reproduction of realistic horizontal and vertical seismic movements.

- Maximum displacement: ±150 mm in each translational direction, allowing the simulation of significant amplitude motions;
- Maximum velocity: up to 0.8 m/s, ensuring the capability to reproduce fast and abrupt earthquake movements;
- Maximum acceleration: approximately 3 g under maximum load conditions, enabling simulation of strong-intensity earthquakes.

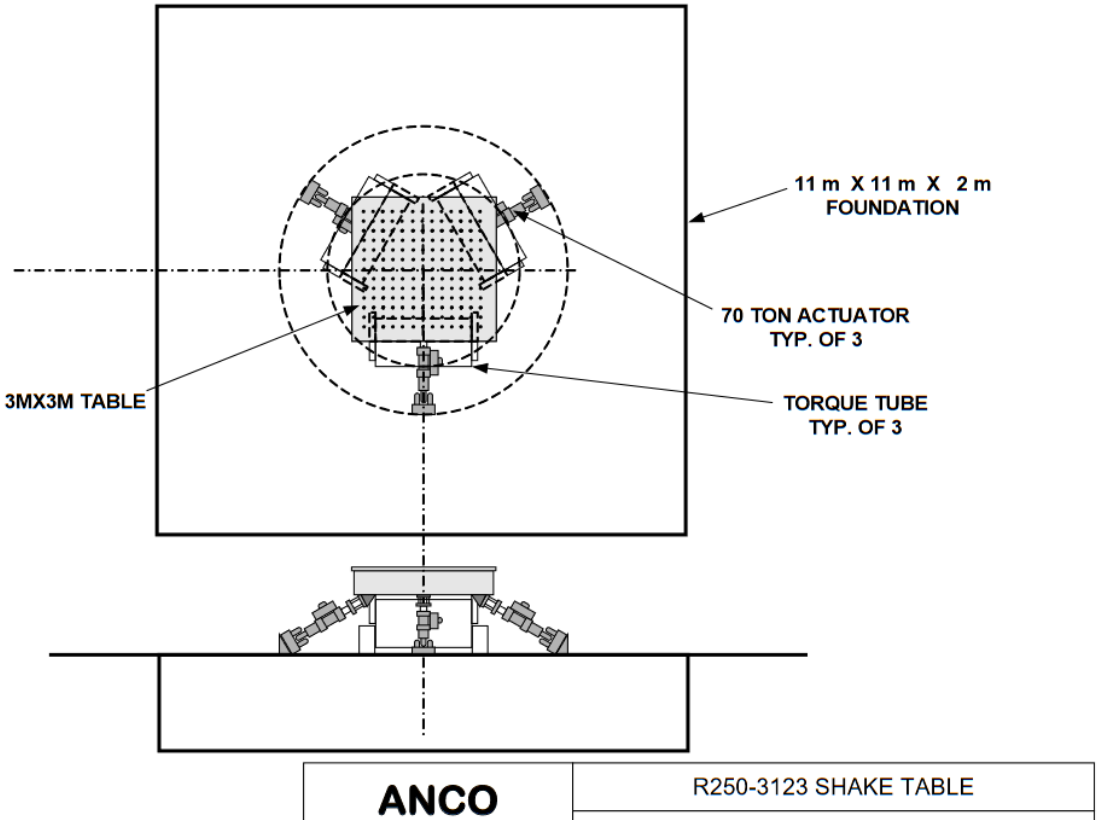

Fig. 8 – Schematic representation of the seismic platform

2. Structural and Loading Capacity

- Steel support frame: plan dimensions of 3 m × 3 m and a maximum height of 5 m;
- Useful payload: up to 16 tons, enabling testing of structural assemblies with various dimensions and weights.

3. Actuation and Control System

The platform is driven by three servo-hydraulic actuators, each with a nominal capacity of 700 kN, providing the necessary force to move the platform under full load. Additionally, three torsional control cylinders maintain the platform's stability by compensating for rotational effects during operation. A real-time displacement control system continuously monitors and adjusts the motion of the platform to ensure faithful reproduction of the programmed seismic scenarios. A dedicated acceleration control system maintains the target acceleration levels during testing, which is essential for the accuracy of results.

4. Signal Generation and Simulation Capabilities

The platform can generate and reproduce a wide variety of waveform signals for actuation, including sinusoidal, pulse, and complex combined signals.
Its operational frequency range extends from 0 to 50 Hz, covering the frequency domain relevant to both earthquake and structural vibration phenomena.

5. Motion Control and Regulation System

The platform is equipped with a triaxial vibration table motion-control system, which synchronizes movements along the three axes, enabling complex, multidirectional seismic simulations.

3.2 Software System and User Interface

The vibration table is operated through a GARDNER SYSTEMS software suite dedicated to motion control and signal generation. This interface allows users to program and execute predefined or custom seismic scenarios, visualize and export results, and perform real-time monitoring of platform parameters. The real-time control interface permits fine adjustments of both displacements and accelerations during operation, ensuring a high degree of repeatability and accuracy for each test.

3.3 Instrumentation and Data Acquisition

3.3.1 Accelerometers

Wireless accelerometers of the type LORD Microstrain G-LINK-200-8G, (https://www.microstrain.com/wireless-sensors/WSDA-200-USB) connected via a WSDA-200-USB acquisition gateway, were used to record structural accelerations (Figure 9). Their positioning is illustrated in Figure 14. These sensors provide high-precision measurements of acceleration on three orthogonal axes and allow synchronized data acquisition from multiple nodes.

Fig. 9a- Wireless accelerometers G-LINK-200-8G

Fig. 9b– Data acquisition system WSDA-200-USB Wireless Gateway

The recorded data were processed using SENSORCONNECT software (Figure 10), developed by *MicroStrain*. This advanced application enables configuration and real-time monitoring of wireless and inertial sensors. It supports large networks of synchronized wireless nodes and allows users to visualize extensive datasets in customizable dashboards.

Data can be exported in CSV format for later analysis or uploaded to the **SensorCloud** platform for additional processing. The software is compatible with devices operating under the MIP protocol and provides functions for filtering, sampling-rate control, and remote access via TCP/IP — a robust solution for industrial and structural monitoring applications. https://www.microstrain.com/software/sensorconnect

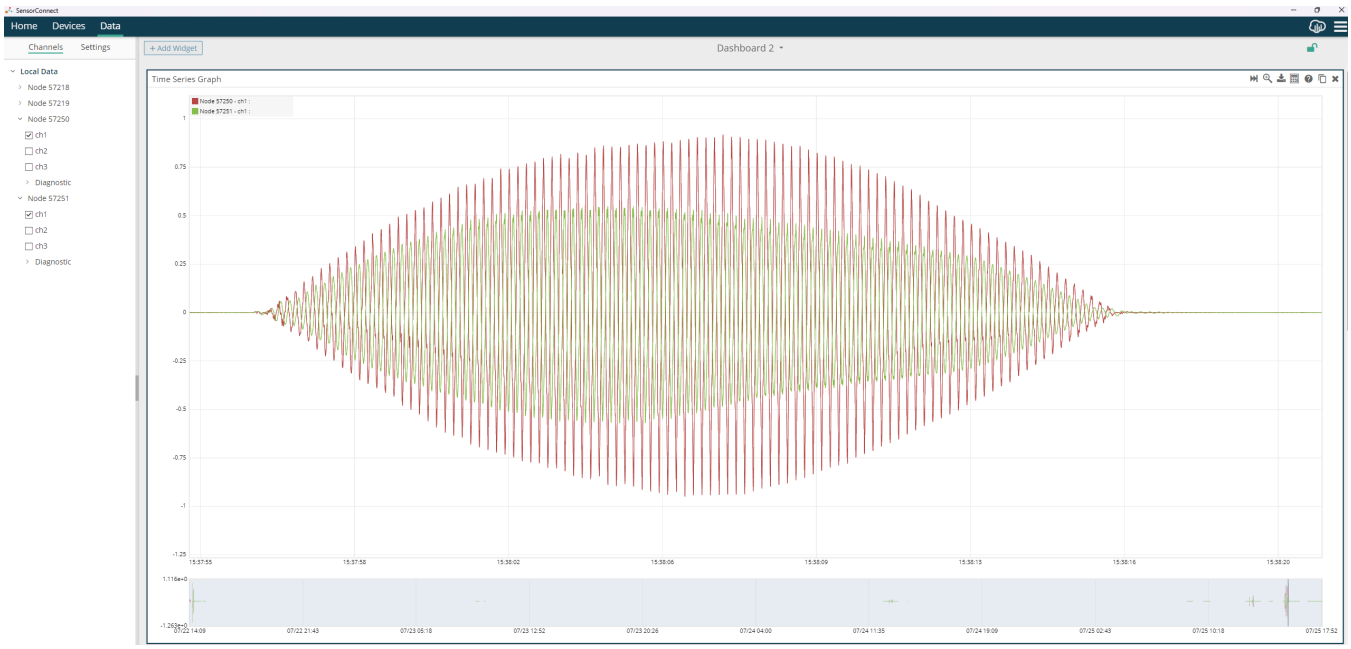

Fig. 10 – SENSORCONNECT software interface

3.3.2 Displacement Transducers

Displacement measurements were obtained using Micro-Epsilon optoNCDT ILR 2250 laser transducers, installed according to Figures 11 and 12. They provide a measurement range up to 100 m (150 m with reflector), high precision, signal stability, ±1 mm linearity, 0.1 mm resolution, and repeatability under 300 µm. The devices feature both analog output and digital interfaces (RS422 / USB / PROFINET / Ethernet/IP / IO-Link) (https://www.micro-epsilon.com/distance-sensors/laser-distance-sensors/optoncdt-ilr2250/)

Fig. 11- LASER displacement transducer optoNCDT ILR 2250

Fig. 12 – Four-channel RS422/USB data acquisition converter IF2004/USB

The transducers were operated using SensorTOOL software (Figure 13), also developed by Micro-Epsilon. This intuitive application facilitates sensor configuration, monitoring, and data recording. It supports real-time visualization and data export, making it ideal for industrial and structural testing applications that require accurate displacement tracking.

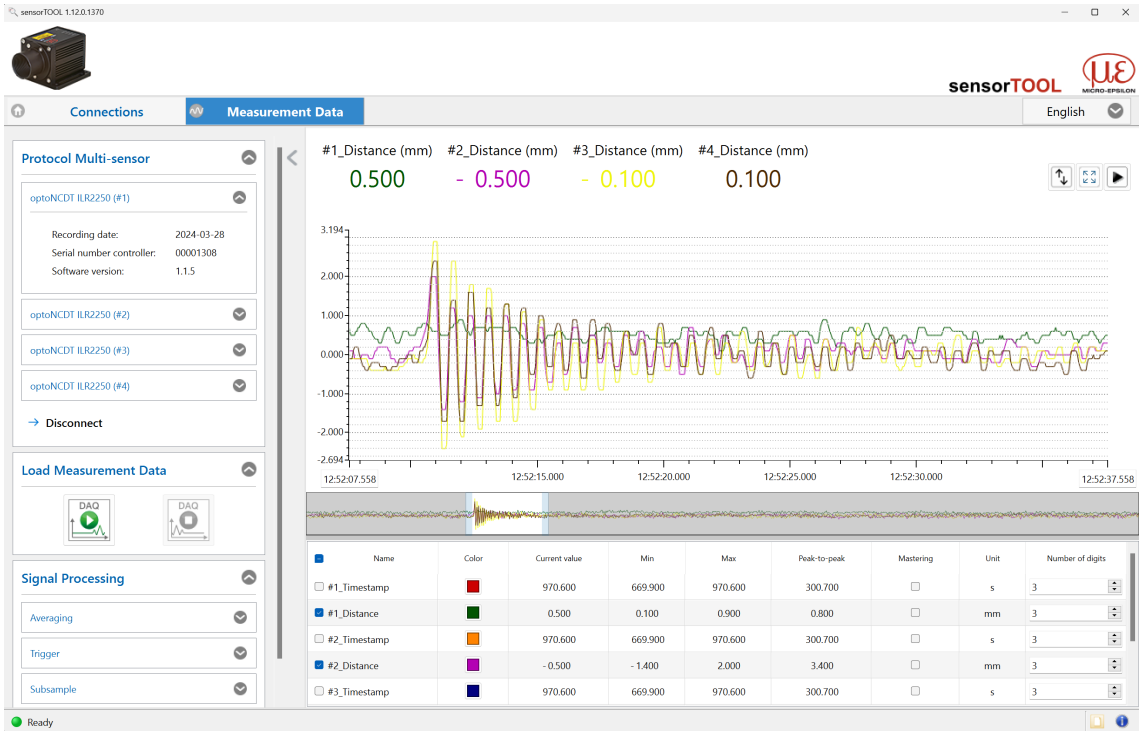

Fig. 13 – SensorTOOL software interface

3.3.3 Position of Sensors

Figure 14 shows the placement of laser displacement transducers and accelerometers at the base of the structure and above the floor slab, while Figure 15 indicates the position of the upper-level sensors. These configurations ensured the synchronized measurement of both absolute and relative motions during each seismic test.

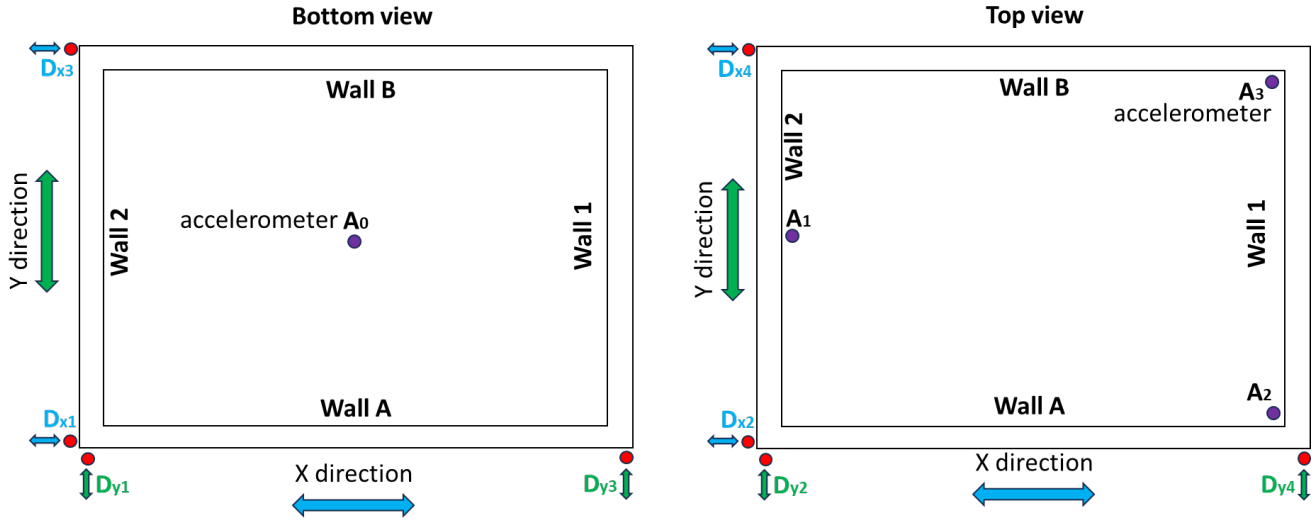

Fig. 14 – Position of displacement transducers and accelerometers at the base and above the floor slab

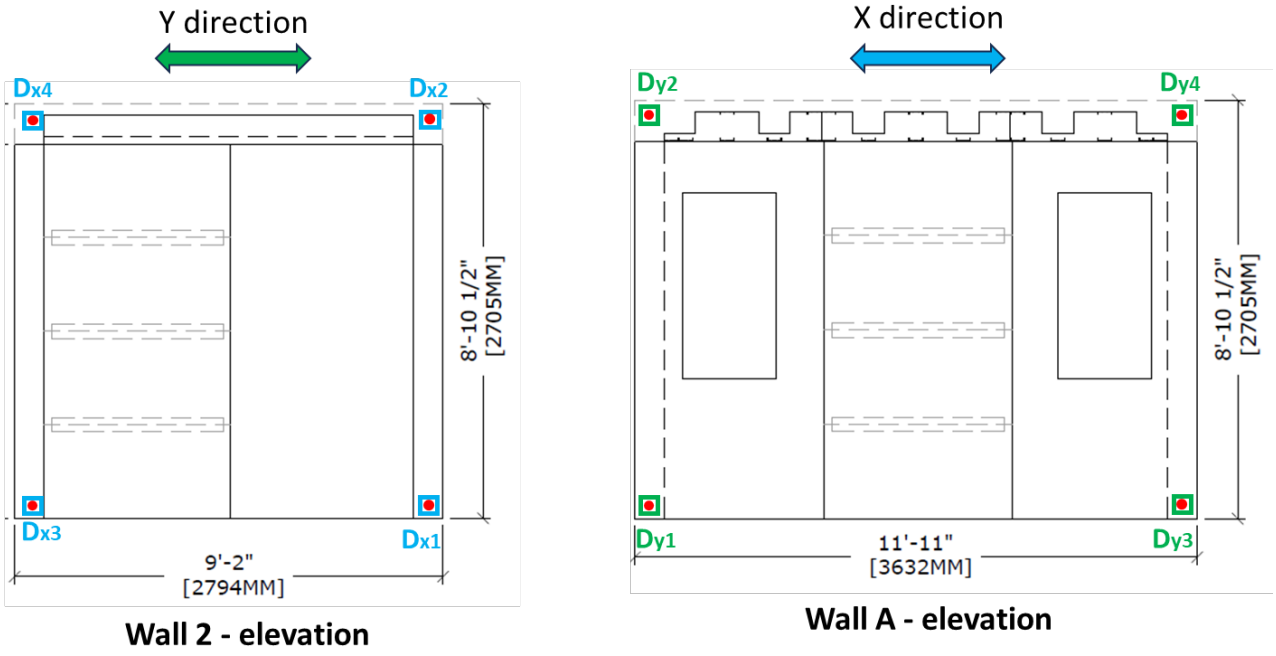

Fig. 15 – Position of LASER displacement transducers at the base and at the top level of the structure

Fig. 16 – Position of accelerometers on the structure

Fig. 17 – Position of LASER displacement transducers on the structure

4 TESTING PROCEDURE

4.1 DETERMINATION OF THE NATURAL FREQUENCIES OF THE STRUCTURE

To identify the dynamic characteristics of the tested models, **Fast Fourier Transform (FFT)** analyses were performed on the measured acceleration signals obtained after a short manual impulse (mechanical shock).

Figure 18 presents the signal recorded by accelerometer A1, from which the FFT spectrum was extracted during the free, unforced vibration phase. This analysis was repeated throughout the testing program, following the chronology shown in Tables 1 and 2.

Fig. 18 - Frequency spectrum (FFT) of accelerometer response after Test D1

4.2 Seismic Actions Used

According to the recommendations of **Eurocode 8 (EN 1998-1)** and **P100-1/2013** regarding performance evaluation of structures under seismic actions, the testing procedure must include both real and artificial accelerograms. These recordings must cover a wide frequency range, have sufficient energy content, and be applied in a sequence that allows the progressive assessment of the structural response.

The experimental campaign consisted of **two testing stages**, each corresponding to one of the tested models:

- **Stage 1** – Model THS 24-388 (steel 0.84 mm, EPS 24 kg/m³)
- **Stage 2** – Model THS 24-389 (steel 1.09 mm, EPS 16.9 kg/m³)

The accelerograms used were taken from real earthquake records (https://esm-db.eu), including Vrancea 1977, Imperial Valley 1979, Northridge 1994, and Turkey 2023. Each accelerogram was scaled to a reference acceleration level of 0.4 g, maintaining the original frequency content.

In Stage 1, the accelerograms were resampled with a smaller time step to increase the high-frequency content of the input motion, thus better matching the tested structure, which exhibited a fundamental frequency of approximately 5 Hz.

In Stage 2, the original accelerograms were used, scaled to a maximum acceleration of 0.4 g. Additionally, five artificial accelerograms were generated according to the design spectrum defined in P100-1/2013, with a peak ground acceleration (PGA) of 0.4 g and a corner period Tc = 1.6 s. Tables 1 and 2 summarize the applied seismic actions and the corresponding maximum accelerations recorded at the seismic platform level.

Table 1. Seismic Actions and Maximum Acceleration Values Generated at Platform Level – Stage 1

Test no.	Tag	Duration [s]	Action type	Frequency [Hz]	PGA X aprox. [g]	PGA Y aprox. [g]
A1	**FFT 0**	5	impulse	**5.04**		
1	T1-AE1	30	artificial earthquake	3 - 25	0.046	0.014
2	T2-AE2	30	artificial earthquake	3 - 25	0.091	0.048
3	T3-AE3	30	artificial earthquake	3 - 25	0.192	0.052
4	T4-AE4	30	artificial earthquake	3 - 25	0.277	0.103
5	T5-AE5	30	artificial earthquake	3 - 25	0.289	0.086
6	T6-AE6	30	artificial earthquake	3 - 25	0.401	0.092
7	T7-AE7	30	artificial earthquake	3 - 25	0.55	0.098
8	T8-AE8	30	artificial earthquake	3 - 25	0.8	0.122
B1	**FFT 1**	5	impulse	**4.70**		
9	T9-SB1	20	sinus beat	5	0.077	0.042
10	T10-SB2	20	sinus beat	5	0.154	0.059
11	T11-SB3	20	sinus beat	5	0.296	0.07
12	T12-SB4	20	sinus beat	5	0.422	0.078
13	T13-SB5	20	sinus beat	5	0.54	0.083
14	T14-SB6	20	sinus beat	5	0.731	0.088
15	T15-SB7	20	sinus beat	5	0.949	0.15
16	R1	30	artificial earthquake SM round 1	1 - 21.7	0.10	0.05
17	R2	30	artificial earthquake SM round 1	1 - 21.7	0.17	0.074
18	R3	30	artificial earthquake SM round 1	1 - 21.7	0.22	0.07
19	R4	30	artificial earthquake SM round 1	1 - 21.7	0.27	0.08
20	R5	30	artificial earthquake SM round 1	1 - 21.7	**0.38**	0.12
21	R6	20	Imperial Valley 1979 modified	0.50 – 8.65	0.07	0.05
22	R7	20	Imperial Valley 1979 modified	0.50 – 8.65	0.09	0.06
23	R8	20	Imperial Valley 1979 modified	0.50 – 8.65	0.10	0.075
24	R9	20	Imperial Valley 1979 modified	0.50 – 8.65	0.174	0.06
25	R10	20	Imperial Valley 1979 modified	0.50 – 8.65	0.25	0.07
26	R11	20	Imperial Valley 1979 modified	0.50 – 8.65	**0.40**	0.072
27	R12	20	Turkey 2023 scaled -round 1	0.31 – 4.66	0.16	0.09
28	R13	20	Turkey 2023 scaled -round 1	0.31 – 4.66	0.23	0.10
29	R14	20	Turkey 2023 scaled -round 1	0.31 – 4.66	0.35	0.12
30	R15	20	Turkey 2023 scaled -round 1	0.31 – 4.66	**0.50**	0.155
C1	**FFT 4**	5	impulse	**4.63**		
31	R16	20	Sinus beat 5 Hz	5	0.06	0.01
32	R17	20	Sinus beat 5 Hz	5	0.1	0.015
33	R18	20	Sinus beat 5 Hz	5	0.17	0.028
34	R19	20	Vrancea 1977 modified	0.33 – 2.55	0.11	0.025
35	R20	20	Vrancea 1977 modified	0.33 – 2.55	0.14	0.027
36	R21	20	Vrancea 1977 modified	0.33 – 2.55	0.188	0.035
37	R22	20	Vrancea 1977 modified	0.33 – 2.55	0.25	0.037
38	R28	20	Turkey 2023 modified -round 2	0.31 – 4.66	0.165	0.085
39	R29	20	Turkey 2023 modified -round 2	0.31 – 4.66	0.25	0.103
40	R30	20	Turkey 2023 modified -round 2	0.31 – 4.66	**0.35**	0.132
41	R31	30	artificial earthquake SM round 2 – Ar02	1-21.7	0.07	0.038
42	R32	30	artificial earthquake SM round 2 – Ar02	1-21.7	0.093	0.041
43	R33	30	artificial earthquake SM round 2 – Ar02	1-21.7	0.14	0.042
44	R34	30	artificial earthquake SM round 2 – Ar02	1-21.7	0.205	0.047
45	R35	30	artificial earthquake SM round 2 – Ar02	1-21.7	0.27	0.07
46	R36	30	artificial earthquake SM round 2 – Ar02	1-21.7	**0.41**	0.08
D1	**FFT 5**	5	impulse	**4.63**		

Table 2. Seismic Actions and Maximum Acceleration Values Generated at Platform Level – Stage 2

Test no.	Tag	Duration [s]	Action type	Frequency [Hz]	PGA X aprox. [g]	PGA Y aprox. [g]
A2		5	impulse	**5.70**		
1	00WN	20	White Noise		0.05	0.03
2	0SS	30	Sine Sweep	0.5 - 7	0.05	0.03
3	1VN	15.355	Vrancea 1977 scaled 50%		0.11	0.04
4	2NHT	40	Northridge 1994 scaled 25%		0.1	0.06
5	3TK	40	Turkey 2023 scaled 25%		0.12	0.07
6	4TKS02	8	Turkey 2023 modified 25%		0.09	0.04
7	5AR02	8	Artificial 0 – scaled 10%		0.09	0.03
8	6Ar1	50	Artificial 1 – scaled 10%		0.093	0.04
9	7Ar2	50	Artificial 2 – scaled 10%		0.091	0.033
10	8Ar3	50	Artificial 3 – scaled 10%		0.092	0.034
11	9Ar4	50	Artificial 4 – scaled 10%		0.089	0.031
12	10Ar5	50	Artificial 5 – scaled 10%		0.11	0.034
B2		5	impulse	**5.30**		
13	00WN	20	White Noise		0.05	0.03
14	0SS	30	Sine Sweep		0.05	0.03
15	1VN	15.355	Vrancea 1977 100%		0.20	0.07
16	2NHT	40	Northridge 1994 scaled 50%		0.22	0.081
17	3TK	40	Turkey 2023 scaled 35%		0.26	0.098
18	4TKS02	8	Turkey 2023 modified 35%		0.18	0.098
19	5AR02	8	Artificial 0 – scaled 50%		0.20	0.07
20	6Ar1	50	Artificial 1 – scaled 20%		0.21	0.071
21	7Ar2	50	Artificial 2 – scaled 20%		0.19	0.068
22	8Ar3	50	Artificial 3 – scaled 20%		0.22	0.076
23	9Ar4	50	Artificial 4 – scaled 20%		0.21	0.07
24	10Ar5	50	Artificial 5 – scaled 20%		0.22	0.076
C2		5	impulse	**4.76**		
25	00WN	20	White Noise		0.05	0.03
26	0SS	30	Sine Sweep		0.05	0.03
27	1VN	15.355	Vrancea 1977 130%		0.26	0.05
28	2NHT	40	Northridge 1994 scaled 100%		0.39	0.14
29	3TK	40	Turkey 2023 scaled 35%		0.23	0.046
30	4TKS02	8	Turkey 2023 modified 35%		0.18	0.098
31	5AR02	8	Artificial 0 – scaled 50%		0.25	0.07
32	6Ar1	50	Artificial 1 – scaled 50%		0.24	0.068
33	7Ar2	50	Artificial 2 – scaled 50%		0.26	0.082
34	8Ar3	50	Artificial 3 – scaled 50%		0.23	0.074
35	9Ar4	50	Artificial 4 – scaled 50%		0.25	0.083
36	10Ar5	50	Artificial 5 – scaled 50%		0.26	0.088
D2		5	impulse	**4.60**		
37	00WN	20	White Noise		0.05	0.03
38	0SS	30	Sine Sweep		0.05	0.03
39	1VN	15.355	Vrancea 1977 130%		0.26	0.05
40	2NHT	40	Northridge 1994 scaled 100%		**0.39**	0.14
41	3TK	40	Turkey 2023 scaled 80%		0.48	0.12
42	4TKS02	8	Turkey 2023 modified 80%		0.43	0.11
43	5AR02	8	Artificial 0 – scaled 80%		0.49	0.13
44	6Ar1	50	Artificial 1 – scaled 80%		0.46	0.12
45	7Ar2	50	Artificial 2 – scaled 80%		0.44	0.10
46	8Ar3	50	Artificial 3 – scaled 80%		0.42	0.11
47	9Ar4	50	Artificial 4 – scaled 80%		0.45	0.12
48	10Ar5	50	Artificial 5 – scaled 80%		0.44	0.11
49	10Ar5	50	Artificial 5 – scaled 100%		**0.61**	0.14
E2		5	impulse	**4.50**		

Figure 19 presents the real earthquake accelerograms obtained from the European Strong-Motion Database (ESM), which were used as input signals in the control software of the seismic platform. The artificial accelerograms, shown in Figure 20, were generated to complement the set of real seismic actions and to enable a comparative analysis of the structural response under equivalent seismic intensity levels.

The main objective was to obtain a set of accelerograms spectrally compatible with the design spectrum defined by P100-1/2013, corresponding to a peak ground acceleration (PGA) of 0.4 g and a corner period Tc = 1.6 s, representative of unfavorable ground type conditions. The artificial accelerograms were obtained through a spectral matching process, using initially generated synthetic records in the 0–20 Hz frequency band, which were subsequently iteratively modified so that the mean response spectrum of the five final records matched the target design spectrum within the relevant period range (0.2–2.0 s).

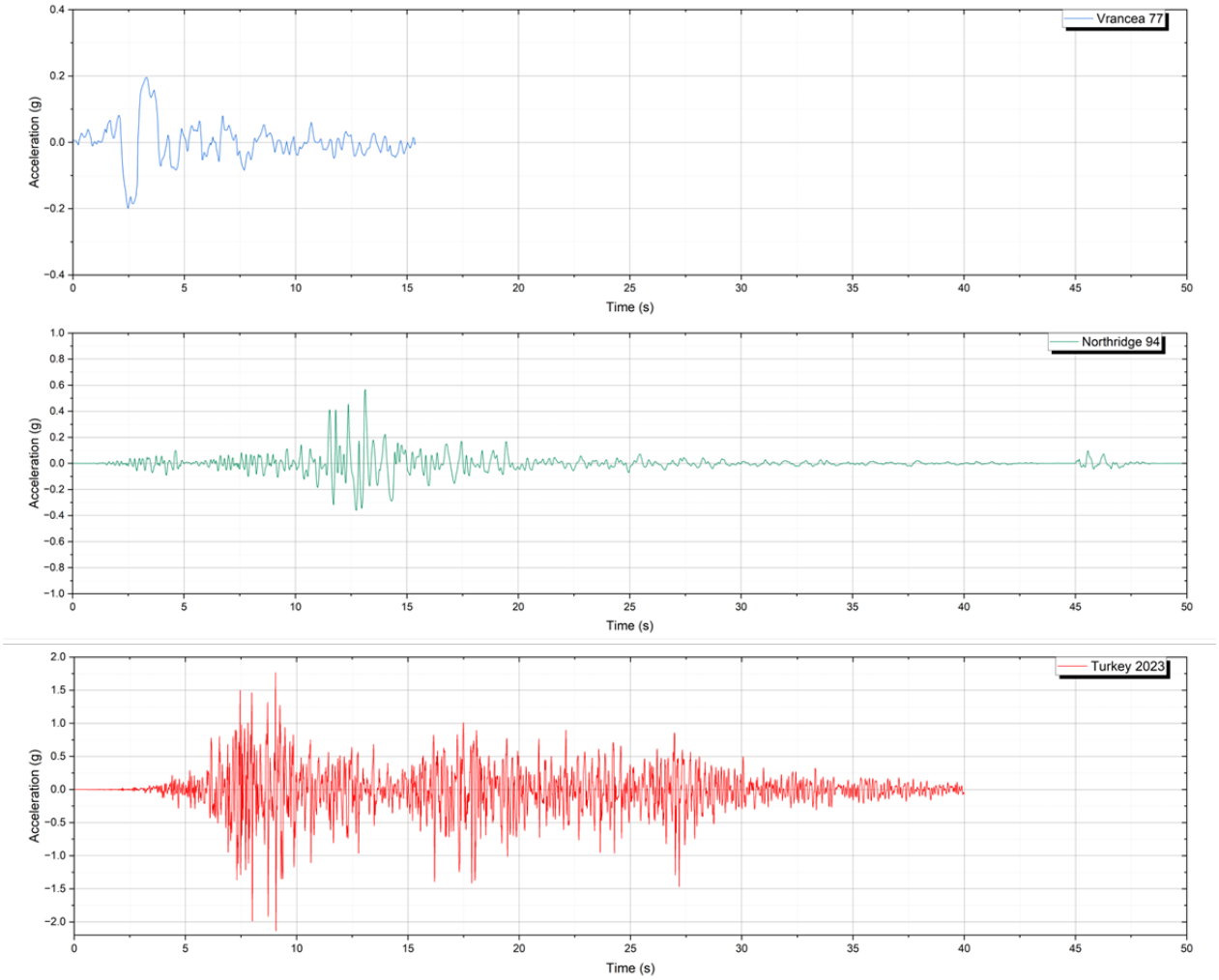

Fig. 19 - Recorded accelerograms of the Vrancea 1977, Northridge 1994, and Turkey 2023 earthquakes.

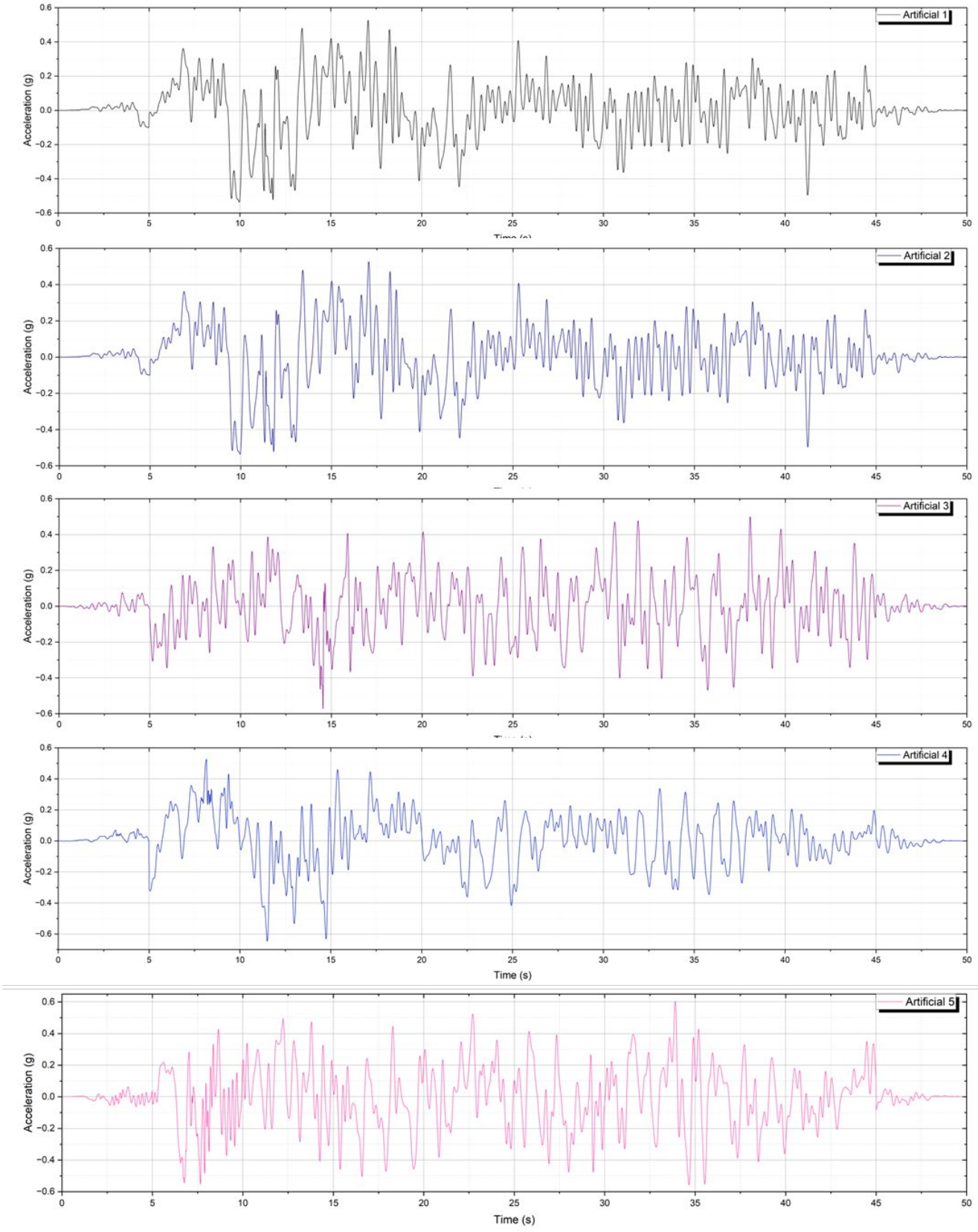

Fig. 20 - Artificial accelerograms

In the final stage, each artificial accelerogram was scaled to a peak amplitude of 0.5 g in order to assess the structure's behavior in the nonlinear range. All signals were standardized to a time step of 0.005 s and a total duration of 50 s, including 5-second ramp-up and ramp-down intervals to prevent initial shocks. Through this procedure, a set of five representative artificial seismic actions was obtained, ensuring a balanced distribution of seismic energy across the entire frequency range relevant to the tested structure.

Figure 21 presents the comparison of the applied action spectra with the target design spectrum (red line), which provides a clear reference for the seismic ground behavior characterized by a corner period Tc = 1.6 s, representative of Romanian soil conditions. The overlaid curves illustrate how the different accelerograms reproduce or exceed this energy level, reflecting the adequacy of the selected input motions relative to the design requirements.

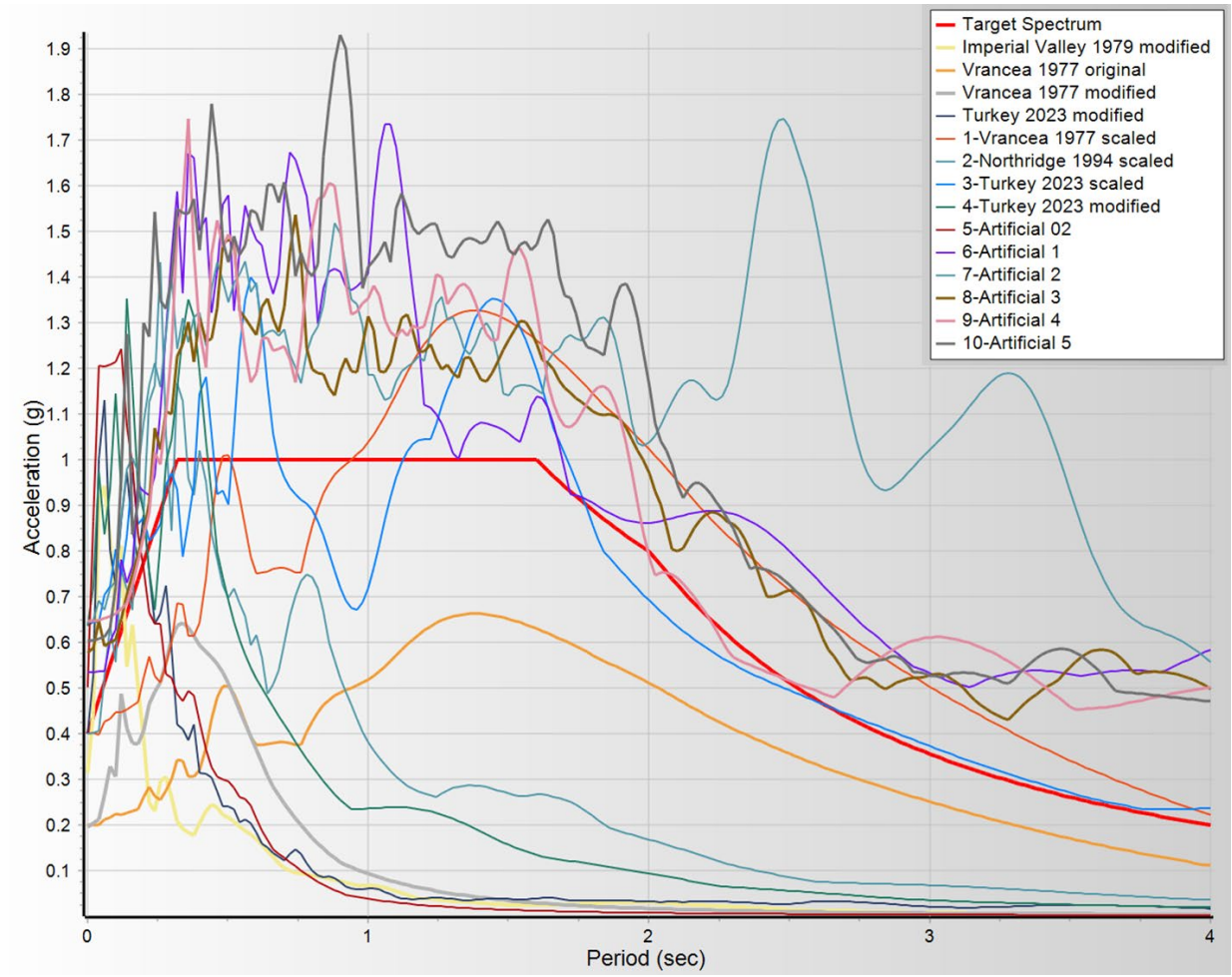

Fig. 21 - Comparison between the response spectra of the applied seismic actions and the target design spectrum according to P100-1/2013 (ag = 0.40 g, Tc = 1.6 s).

The purpose of this comparison is to verify how well the selected set of accelerograms conforms to the Romanian design spectrum specified in code P100-1/2013, corresponding to a peak ground acceleration ag = 0.40 g and a corner period Tc = 1.6 seconds. The analyzed structure, built from Thermasteel panels, has a fundamental frequency of about 5 Hz, which corresponds to a natural period $T_1 \approx 0.20$ seconds. This indicates a stiff structural behavior that is particularly sensitive to short-period spectral components.

The design spectrum, shown by the red curve, maintains a constant plateau up to T ≈ 1.6 seconds, followed by a gradual decay of accelerations. The analysis of the curves shows that most real accelerograms exceed the target spectrum in the range of T = 0.1–0.3 seconds, which is advantageous when testing a short-period structure. The maximum spectral values reach levels between 1.3 and 1.9 g, ensuring a sufficiently severe excitation. For longer periods (T > 1.6 seconds), some records fall below the design spectrum, which is acceptable since the influence of this range on the tested structure is limited.

The artificial accelerograms (1–5) reproduce the target spectral shape accurately, covering uniformly the 0.2–2.0 second period range and compensating for the irregularities of the natural motions. This results in a complete and balanced representation of the seismic demand over the entire range of relevant structural periods.

4.3 JUSTIFICATION OF THE SELECTED ACTIONS

4.3.1 Compliance with Local Seismic Hazard

The real accelerograms used in the testing program were scaled so that their maximum base acceleration reached a value of 0.40 g, corresponding to the design ground acceleration defined in the Romanian seismic code P100-1/2013. In addition, the adjusted versions were spectrally corrected to match as closely as possible the target design spectrum associated with a corner period Tc = 1.6 s, representative of Romanian soil type C–D. This approach ensured that the imposed actions accurately reflected the seismic hazard level for which the Thermasteel structural system is intended.

4.3.2 Representation of Different Earthquake Types

The selected accelerograms cover a wide variety of seismic sources and frequency contents, ensuring a realistic simulation of different ground motion types. The Vrancea 1977 record represents a deep-focus subcrustal event typical for the Romanian region, characterized by long-duration shaking. The Northridge 1994 and Turkey 2023 records correspond to shallow crustal earthquakes with strong energy concentration in the short-period range, while the Imperial Valley 1979 record represents an intermediate case with moderate duration and a broad spectral content.

This diversity allows the evaluation of the structural response under multiple excitation mechanisms, from long-period to short-period dominant motions. By including both types, the tests reproduce realistic conditions for assessing the performance of a lightweight, stiff structural system such as Thermasteel.

4.3.3 Suitability for the Structural Characteristics of the Tested Model

The Thermasteel structure is characterized by low mass, high stiffness, and a fundamental frequency of about 5 Hz, corresponding to a natural period of approximately 0.20 seconds. Such behavior classifies the system as rigid, making it particularly sensitive to short-period components of the ground motion.

For this reason, accelerograms that amplify the response within the range T = 0.1–0.3 s were intentionally selected. The combination of scaled real records and spectrally matched artificial accelerograms ensures that the excitation energy is concentrated around the structural period of interest, which is critical for accurately evaluating stiffness degradation and potential nonlinear effects.

The applied accelerograms are thus representative of strong-motion scenarios acting on stiff, lightweight buildings, providing a consistent and realistic basis for assessing the seismic performance of the Thermasteel system.

5 EXPERIMENTAL RESULTS

The structural response during each test was monitored and recorded using accelerometers and displacement transducers. The collected data include: absolute accelerations in g (where g is gravitational acceleration) along the longitudinal X and transverse Y directions; absolute displacements in millimeters, indicating the total motion of the structure relative to the fixed positions of the transducers; and interstory (relative) displacements representing the differences in displacement between the levels of the structure.

5.1 RESPONSE TO SEISMIC ACTIONS – MODEL THS 24-388.

Table 3 presents the maximum values of displacements and accelerations in the X direction for the actions relevant to the THS 24-388 structural model.

Table 3 – Maximum accelerations and displacements in the X direction for structural model 1: THS 24-388

Test	Level	Action	Structural response		
		Peak Acceleration X (g)	Peak Acceleration X (g)	Absolute Displacement X (mm)	Maximum Relative Displacement X (mm)
20 R5-Artificial Ar02	Top		0.92	15	8
	Base	0.38		7	
30 R15-Turkey 2023 modified	Top		1.21	26	11
	Base	0.50		15	
37 R22-Vrancea 1977 modified	Top		0.63	23	12
	Base	0.25		11	
40 R30-Turkey 2023 modified	Top		1.04	21	**13**
	Base	0.35		8	
46 R36-Artificial Ar02	Top		1.05	23	**18**
	Base	0.41		5	

5.2 STRUCTURAL RESPONSE TO SEISMIC ACTIONS – MODEL THS 24-389

Table 4 presents the maximum values of displacements and accelerations in the X direction for the actions relevant to the THS 24-389 structural model.

Table 4 – Maximum accelerations and displacements in the X direction for structural model 2: THS 24-389

Test	Level	Action	Structural response		
		Peak Acceleration X (g)	Peak Acceleration X (g)	Absolute Displacement X (mm)	Maximum Relative Displacement X (mm)
40 Vrancea 1977 scaled 130%	Top		0.49	10	7
	Base	0.26		3	
41 Northridge 1994 scaled 100%	Top		0.92	34	26
	Base	0.39		12	
43 Turkey 2023 modified 80%	Top		1.23	43	28
	Base	0.43		15	
48 Artificial 5 – scaled 80%	Top		1.28	78	30
	Base	0.44		48	
49 Artificial 5 – scaled 100%	Top		**1.45**	119	**53**
	Base	**0.61**		66	

Fig. 22 Acceleration–time plot in the X direction for action - Artificial 5 scaled 100%.

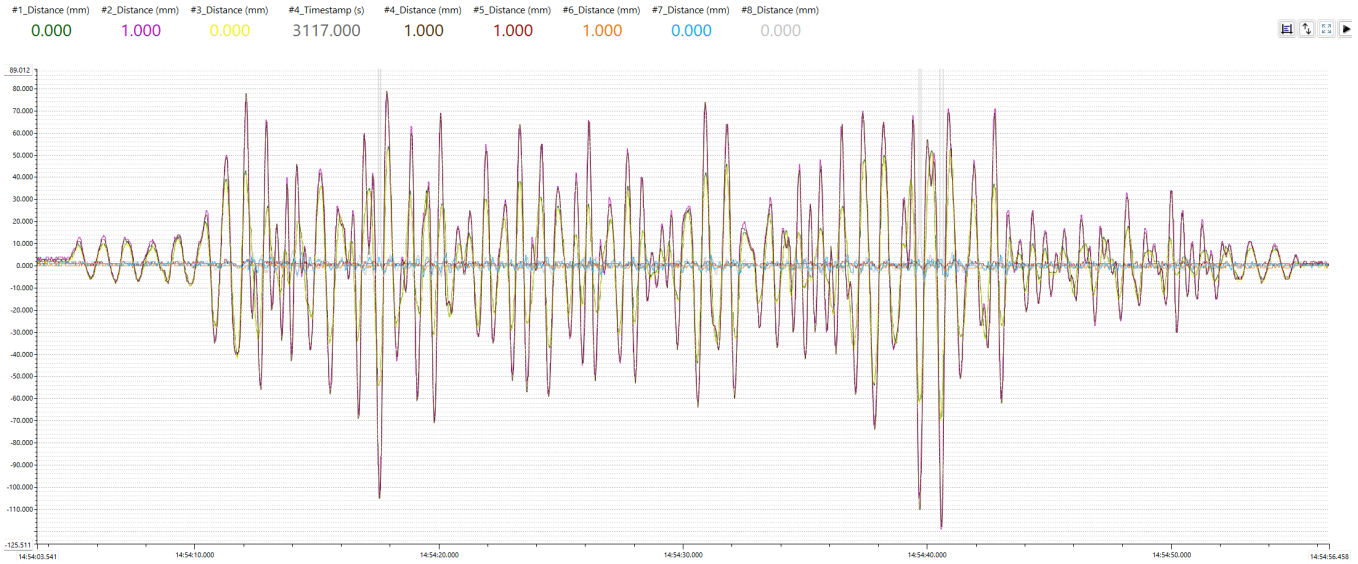

Fig. 23 Absolute displacement–time plots in the X and Y directions for action - Artificial 5 scaled 100%.

5.3 ANALYSIS OF STRUCTURAL BEHAVIOR

5.3.1 Evolution of the fundamental natural frequency

For model THS 24-388, the initial frequency was 5.04 Hz. After the first series of tests it gradually decreased to 4.70 Hz, indicating a slight stiffness loss. At the end of all tests, the frequency decreased again slightly to 4.63 Hz. No significant permanent degradation was recorded; the global stiffness was essentially preserved. For model THS 24-389, the initial frequency was 5.70 Hz, then after the first loading level at 10% scaled actions it dropped to 5.30 Hz. After the 20% level it fell to 4.76 Hz. Following the 50% level it reached 4.60 Hz. In the final stage, after action Artificial 5 at 100% with a maximum acceleration of 0.61 g, the fundamental frequency was 4.50 Hz. This nearly 22% reduction relative to the initial value shows that some screw-fastened joints exhibited loosening, a fact also observed visually and documented in photographs.

5.3.2 Determination of the fraction of critical damping

The analysis was performed on the impulse response of channel A2 (upper level), which has the best signal-to-noise ratio. Peaks of the same sign were extracted from the free-decay phase after the impulse maximum, and the logarithmic decrement method was applied. For two successive peaks, the decrement is given by relation (1). The relative damping is evaluated with relation (2), where the decrement is averaged over the first 10–12 peaks. The period was obtained from the time distance between successive peaks. With the total mass, the critical damping is , and the equivalent viscous damping is . On the free damped-vibration window: initial natural frequency: ; initial fraction of critical damping: 1.52%; final fraction of critical damping: 1.53%.

$$\delta_i = \ln\left(x_i / x_{i+1}\right). \quad (1)$$

critical damping:

$$\xi \approx \frac{\bar{\delta}}{2\pi}, \tag{2}$$

where $\bar{\delta}$ epresents the average of the logarithmic decrements over the first 10–12 peaks. The vibration period was obtained from the time interval between successive peaks, with the natural frequency calculated as $f_n = 1/T$. Considering the total mass $m = 4500$ kg, the critical damping $c_{\text{crit}} = 2\, m\, \omega_n$, $\omega_n = 2\pi f_n$, nd the equivalent viscous damping is $c = \xi\, c_{\text{crit}}$.

On the time window corresponding to the free damped vibration:

- initial natural frequency: $f_n = 5.700$ Hz ($T = 0.175$ s);
- initial fraction of critical damping: ξ ≈**1.52% inițial**;
- final fraction of critical damping: $\xi \approx$ **1.53% final**.

5.3.3 Force–displacement curve

The nonlinear response of the structure was evaluated by plotting the base seismic force versus relative displacement (Fig. 24), obtained from the accelerograms measured at the base and at the top of the model. The force was computed as the product of the total mass of the structure (4,500 kg) and the relative acceleration (difference between the accelerations measured at the top and at the base). The relative displacement was determined from the difference of the translation signals measured at the same points, and the data were filtered with a 12 Hz Butterworth low-pass filter to remove high-frequency noise.

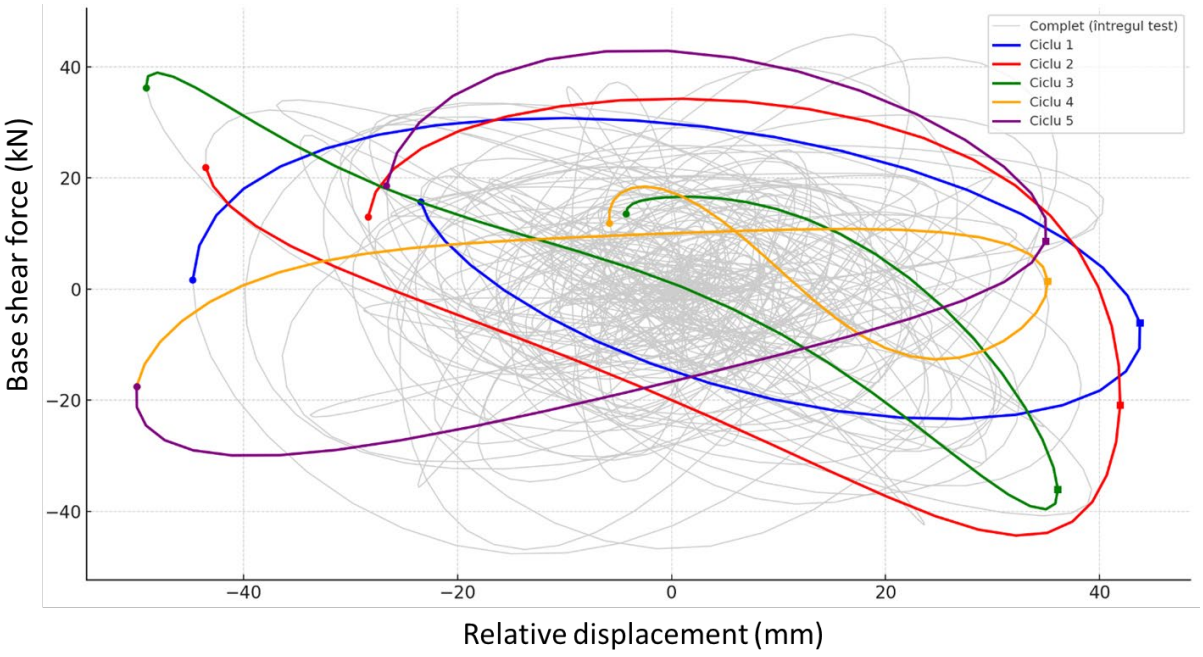

Fig. 24 Base shear force versus relative displacement for action 49 – Artificial 5 scaled 100%.

Figure 24 shows the five most representative complete hysteresis loops, superimposed on the global response of the structure. The gray curve represents the complete response, while the colored loops correspond to the cycles in which maximum displacement and force were reached. Each loop describes a full loading–unloading cycle, from

maximum negative to maximum positive displacement and back. The slender, nearly linear shape of the loops indicates predominantly elastic behavior of the Thermasteel system, with low energy losses and a small equivalent damping (ξ ≈ 1.5%). The absence of a wide loop or pinching shows that no significant plastic deformations occurred; energy dissipation took place mainly through local friction mechanisms and reversible deformations at the joints. The uniform distribution of cycles and the near-complete return to the initial position after each unloading confirm the stability of the system and the good quality of the panel-to-panel and wall-to-base connections. The global response remained stable, with no evident stiffness drop between successive cycles.

5.4 VERIFICATION OF INTERSTORY DRIFT

Lateral drift verification is essential for evaluating serviceability and global stability. At the serviceability limit state (SLS), comfort and the integrity of non-structural elements (walls, plasters, finishes) are assessed. Exceeding SLS indicates the possibility of fine cracking, local detachments, or aesthetic degradation, but does not affect structural safety. At the ultimate limit state (ULS), global deformation and the risk of loss of stability are controlled. The condition $\delta_{\max} < 0.025 \cdot h$ confirms that the structure did not reach the ultimate limit state and the global behavior remains structurally safe.

According to design code P100-1/2013, Annex E, the admissible limits are: SLS – 0.005·h = 13.5 mm (for brittle nonstructural elements such as plaster and masonry) and 0.008·h = **21.6 mm** (for non-brittle components that do not interact with the structure); ULS – 0.025·h = **67.5 mm**.

For the story height h = 2705 mm, in the THS 24-389 model under action 49 – Artificial 5 scaled 100%, with a maximum acceleration of 0.6 g, the maximum interstory displacement is 53 mm, as given by relation (3).

$$\frac{\delta_{\max}}{h} = \frac{\mathbf{53}}{2700} = 0.0196 \approx 1.96\% \tag{3}$$

Results of the checks:

- $\delta_{\max} = 53$ mm**>** 21.6 mm → **SLS is exceeded**.
- $\delta_{\max} = 53$ mm**<** 67.5 mm → **ULS is satisfied**.

Table 5 summarizes the representative interstory relative displacement values obtained from the most demanding seismic actions.

Table 5. Summary of interstory drifts compared to admissible values

Tested structure	Maximum acceleration (g)	Experimental test Maximum interstory drift (mm)	SLS – admissible maximum drift *0.008h=21.6* (mm)	ULS – admissible maximum drift *0.025h=67.5* (mm)
THS 24-388	0.25	12	<	<
	0.35	13	<	<
	0.41	18	<	<
THS 24-389	0.26	7	<	<
	0.44	30	>	<
	0.61	**53**	>	<

5.5 VISUAL OBSERVATION OF DAMAGE

During the experimental tests on models THS 24-388 and THS 24-389, the following observations regarding the occurrence of damage were made. After each stage of seismic actuation, visual inspections were carried out (Figs. 25–33). For THS 24-388, where the maximum acceleration level was 0.41 g and the maximum interstory drift was 18 mm, no loosening of connections or other types of local or global damage were observed. During testing, local vertical displacements were noticed between the reinforced concrete slab and the top track of the walls, without leading to visible subsequent damage (Figs. 34, 35).

For THS 24-389, after the last dynamic action corresponding to artificial accelerograms scaled to 100% (peak acceleration 0.61 g) and an interstory drift of approximately 53 mm, the following were observed.

5.5.1 Local deformation and loosening of mechanical joints.

In the panel-to-panel splice zones (two adjacent panels connected by steel splice plates with three self-tapping screws per panel – see Fig. 38), outward movement of some screws and partial rotations (unthreading) were observed. The holes around these screws were slightly deformed, with a visible increase in diameter, indicating local plastic deformations and reduced bearing contact between screw and sheet. The number of such defects is low, affecting approximately 1% of all screws in the assembly.

Figs. 25–33. Post-test details for model THS 24-388 (upper and lower parts of wall A, window opening detail, door opening base detail on wall B, exterior corner detail walls B / wall 1, interior upper and base details, interior connector details and window opening). Figs. 34–35. Video frame details of wall B, model THS 24-388, during Turkey 2023 action – leftward and rightward motion.

Fig. 25 Upper part of wall A – structural model THS 24-388 after completion of the tests.

Fig. 26 Lower part of wall A – structural model THS 24-388 after completion of the tests.

Fig. 27 Window opening detail on wall A – structural model THS 24-388 after completion of the tests.

Fig. 28 Door opening base detail on wall B – structural model THS 24-388 after completion of the tests.

Fig. 29 Exterior corner base detail between walls B and 1 – structural model THS 24-388 after completion of the tests.

Fig. 30 Interior detail, upper part of walls B and 1 – structural model THS 24-388 after completion of the tests.

Fig. 31 Interior detail, base of walls B and 1 – structural model THS 24-388 after completion of the tests.

Fig. 32 Interior connector detail on wall B – structural model THS 24-388 after completion of the tests.

Fig. 33 Interior connector and window opening detail on wall B – structural model THS 24-388 after completion of the tests.

Fig. 34 Video frame detail of wall B, model THS 24-388, during the Turkey 2023 action – motion to the left.

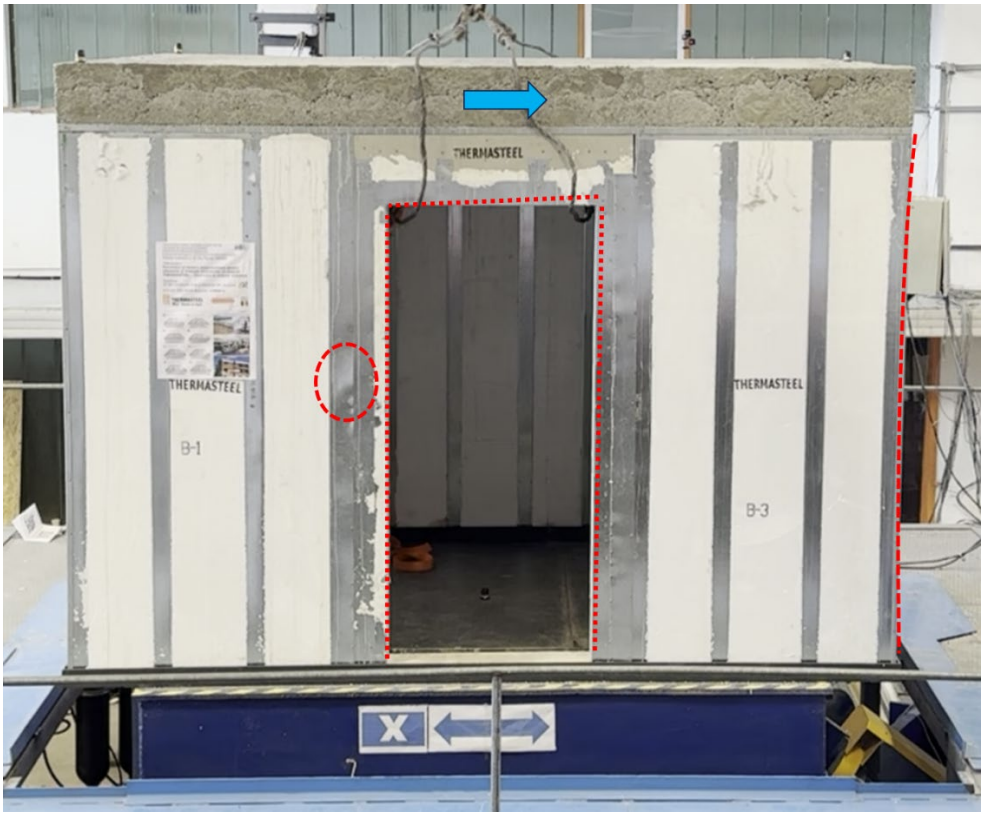

Fig. 35 Video frame detail of wall B, model THS 24-388, during the Turkey 2023 action – motion to the right.

5.5.2 Partial loss of adhesion between the EPS core and the steel faces

At the panel base, near the lower track, a slight local detachment between the expanded polystyrene core and the steel faces was noticed, caused by repeated deformations and rotation at the panel base. Figs. 36–45. Post-test details for model THS 24-389: lower and upper panel joints on wall A (interior/exterior), exterior joints on wall B (upper left/right, lower right), door opening detail after Artificial 1 at 80%, exterior joints at the base of walls 1 and 2 and corner with wall A, all showing the localized effects described above.

5.5.3 Affecting the splice plates between panels

The two main panel joints proved to be the most stressed, exhibiting slight deformations of the splice sheets and slight loosening of several screws (Figs. 36, 37). On the long exterior splice plates, in the door opening area, loosening and slight deformations of the lintel profiles were observed (Figs. 38–41).

Fig. 36 Lower joint between panels on wall A (interior view) – structural model THS 24-389 after completion of the tests.

Fig. 37 Upper joint between panels on wall A (exterior view) – structural model THS 24-389 after completion of the tests.

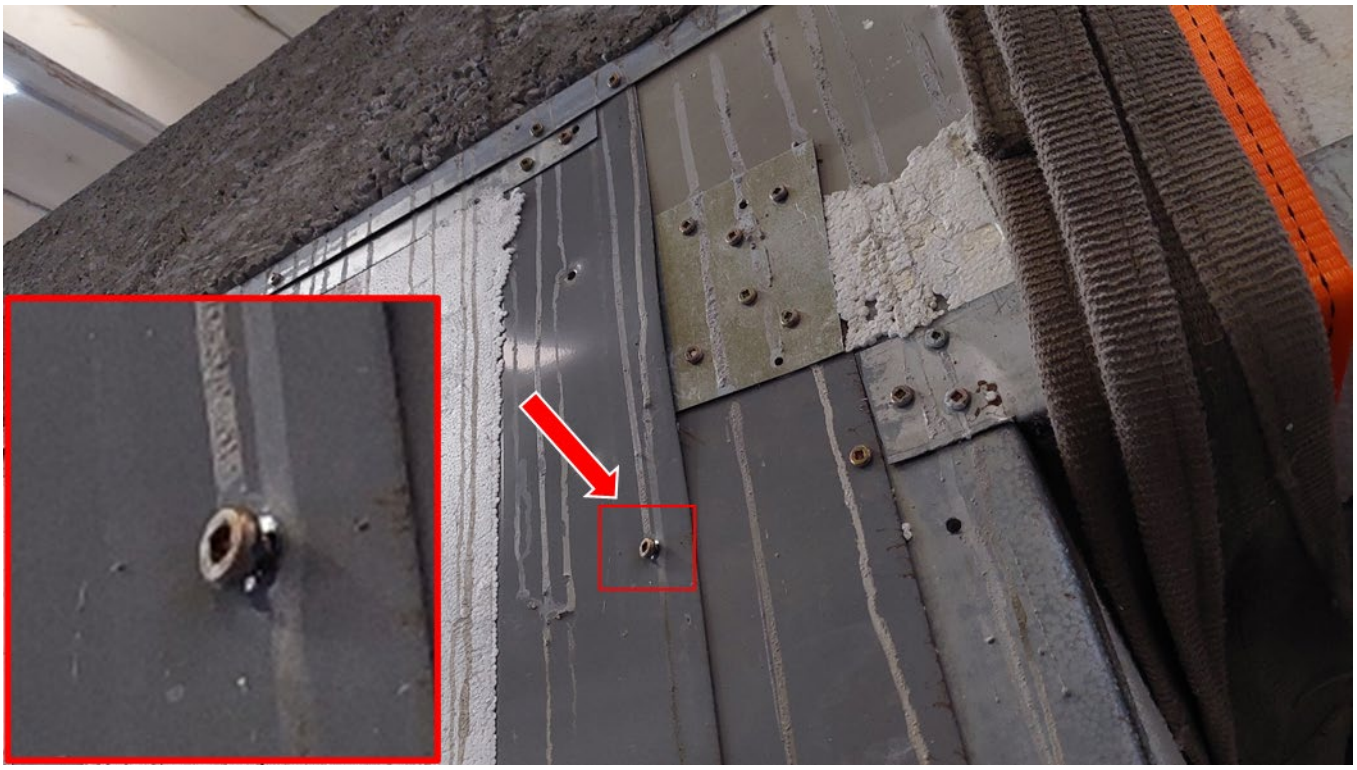

Fig. 38 Exterior joint between panels on wall B (upper left area) – structural model THS 24-389 after completion of the tests.

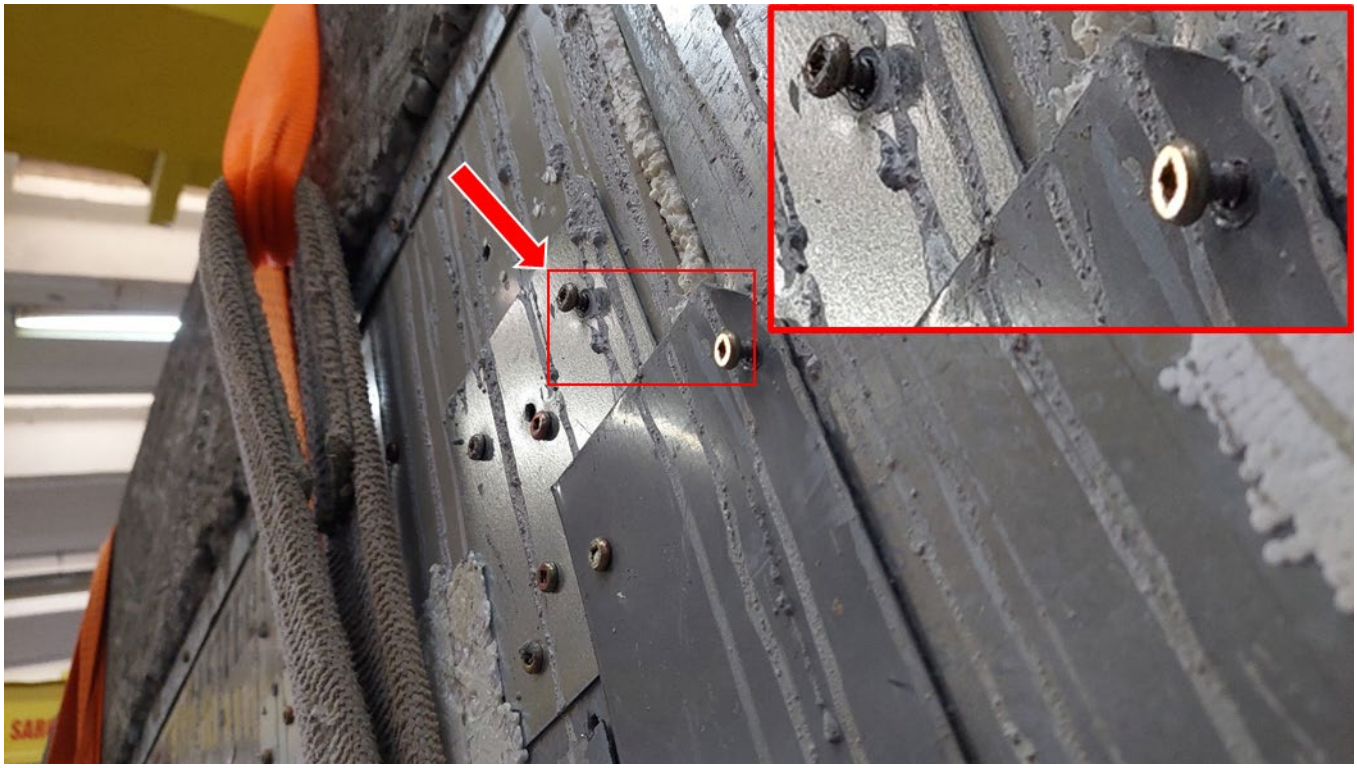

Fig. 39 Exterior joint between panels on wall B (upper right area) – structural model THS 24-389 after completion of the tests.

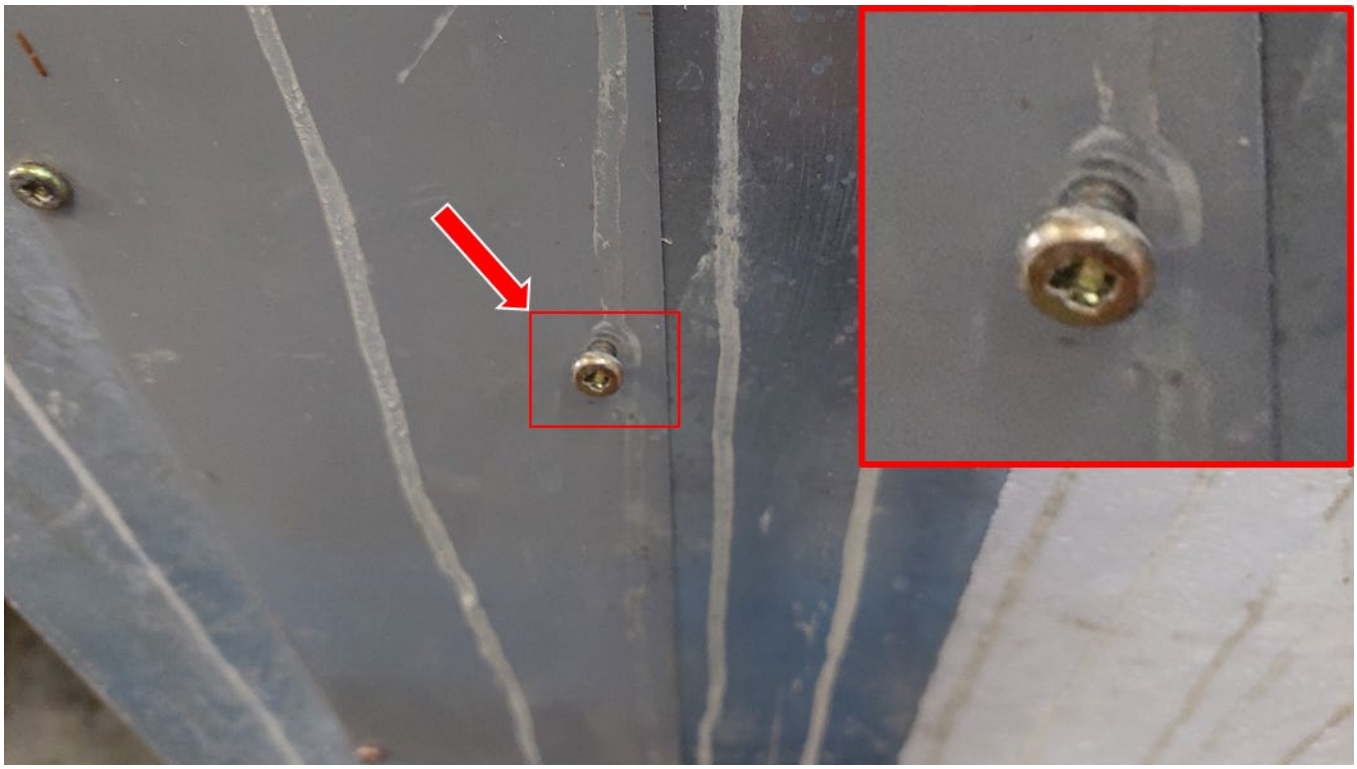

Fig. 40 Exterior joint between panels on wall B (lower right area) – structural model THS 24-389 after completion of the tests.

Fig. 41 Door opening detail on wall B after action Artificial 1 scaled to 80% – structural model THS 24-389.

5.5.4 Local deformation at the base of the walls

In the contact zone between the panels and the lower U-track (base shoe) – Figs. 42–45 – local deformations of the track flanges were observed, especially at the anchorage of vertical studs. Slight screw rotations were also recorded, indicating combined shear and withdrawal demand.

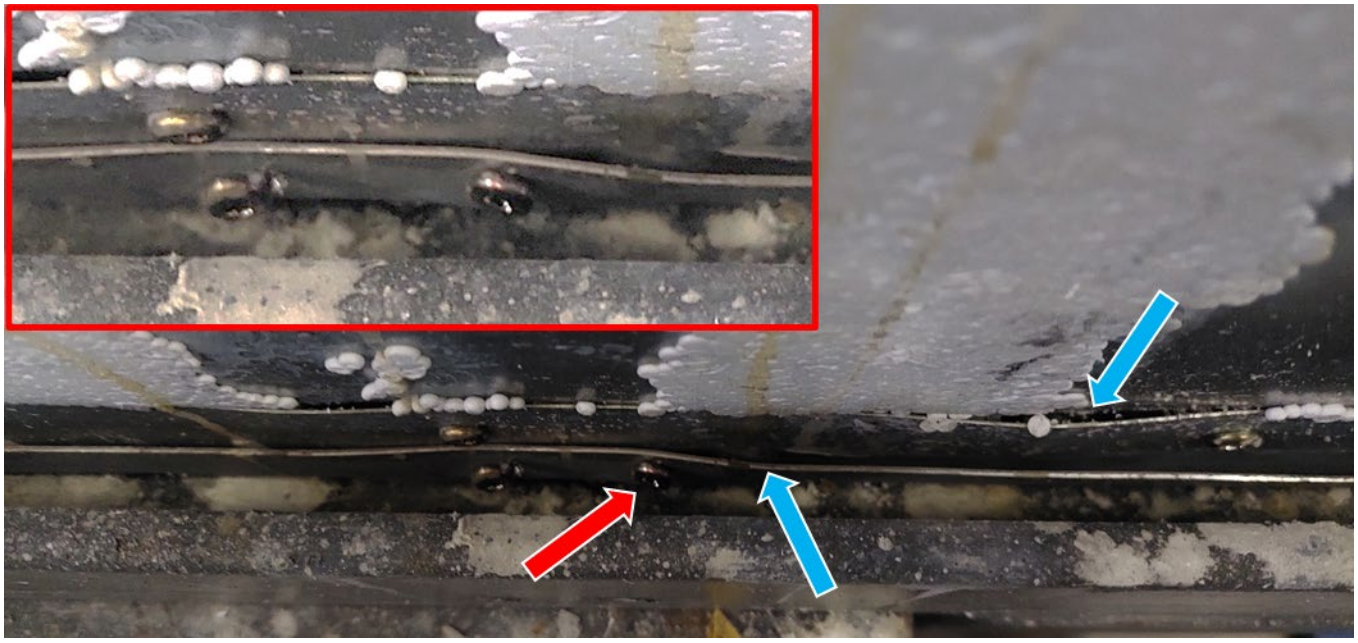

Fig. 42 Exterior joint at the base of wall 1 – structural model THS 24-389 after completion of the tests.

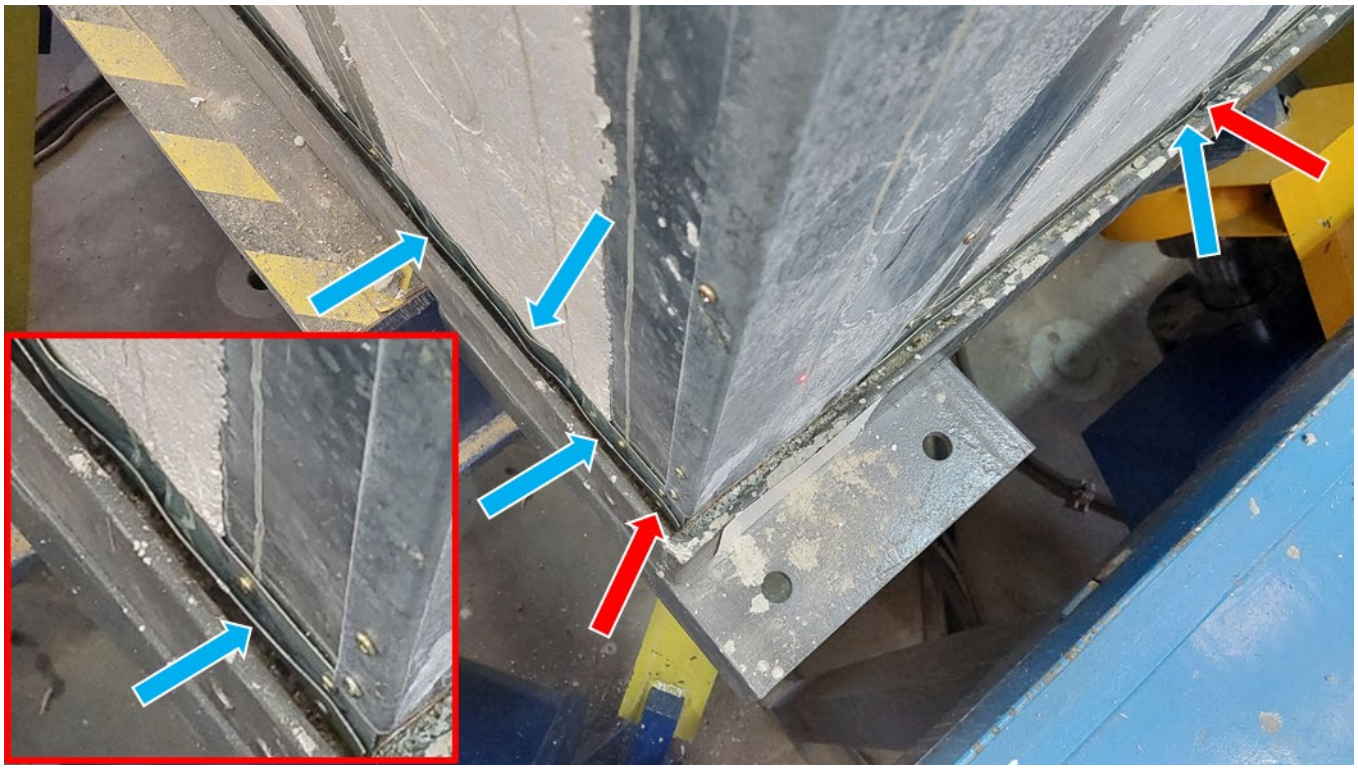

Fig. 43 Exterior joint at the base of wall 2 – structural model THS 24-389 after completion of the tests.

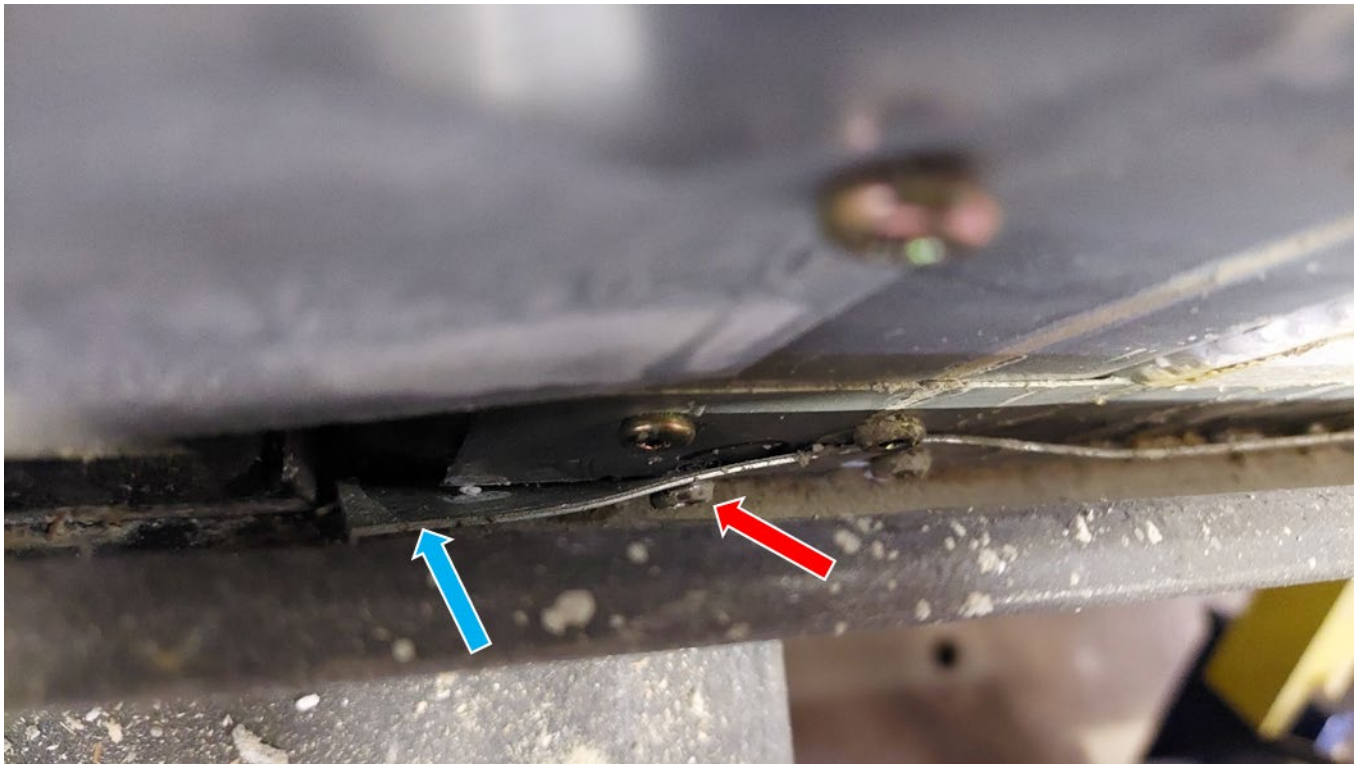

Fig. 44 Exterior corner joint between wall 1 and wall A (base area) – structural model THS 24-389 after completion of the tests.

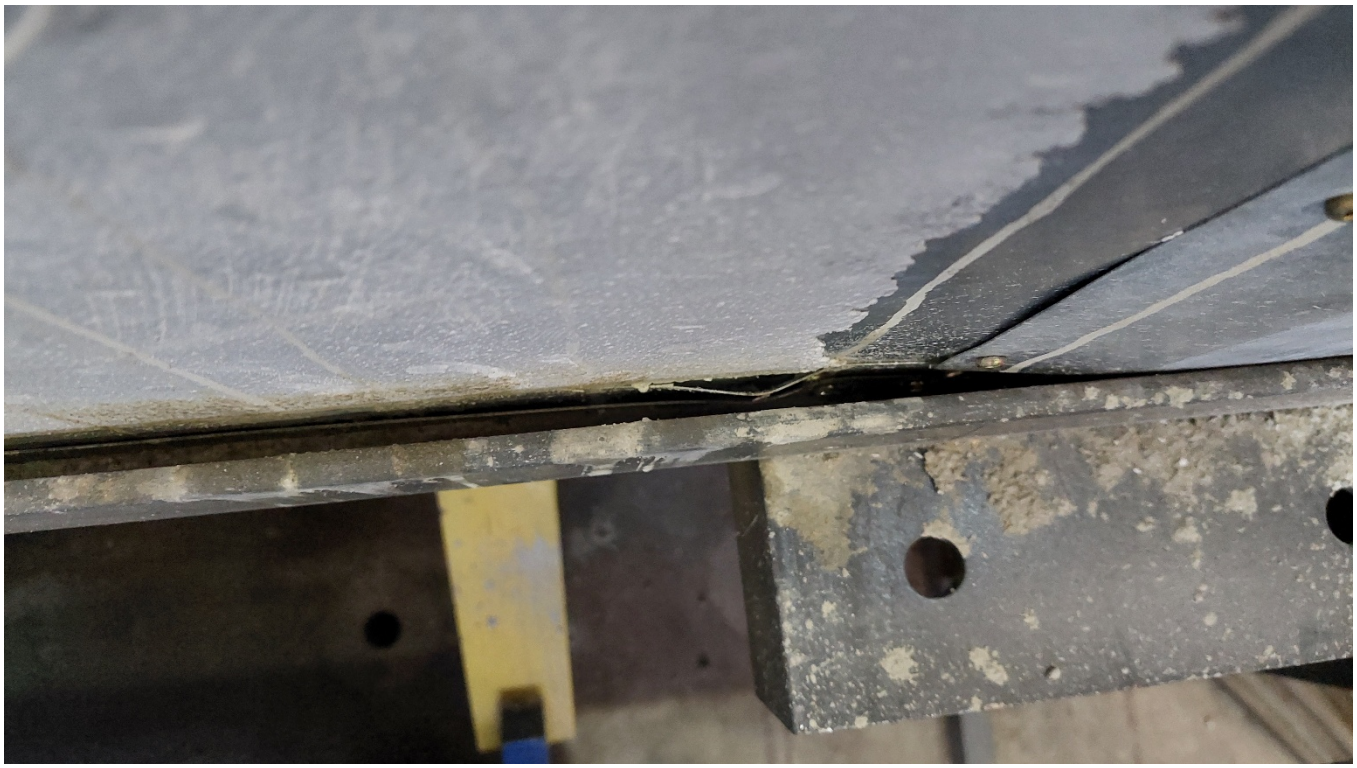

Fig. 45 Detail of the base area of wall A – structural model THS 24-389 after completion of the tests.

6 DISCUSSIONS AND INTERPRETATIONS

6.1 EVOLUTION OF STIFFNESS AND FUNDAMENTAL NATURAL FREQUENCY

The analysis of the results obtained from the dynamic tests shows a significant variation in the fundamental natural frequency of the structure, from initial values of approximately 5.7 Hz (determined from the initial impulse) to values between 4.6 and 4.8 Hz after all seismic actions were applied, in the case of model THS 24-389, built with steel profiles of 1.09 mm thickness and an expanded polystyrene (EPS) core with a density of 16.9 kg/m³. This reduction of approximately 20% indicates a decrease in the effective stiffness of the system, which can be explained by the occurrence of small nonlinearities in the connection zones between panels and at the base anchorage. The phenomenon is typical of lightweight structures, where stiffness depends on the combined behavior of the panel–connector–floor assembly. As the loading cycles are repeated, the perfect contact between components diminishes, and the system transitions from a strictly elastic response to a semi-rigid one, while maintaining stability and reversible deformation.

In the case of model THS 24-388, with steel profiles 0.84 mm thick and an EPS core of 24 kg/m³ density, the initial fundamental frequency was 5.04 Hz and decreased to 4.63 Hz after testing, corresponding to an 8% reduction. This decrease is consistent with the seismic actions applied, characterized by shorter periods (up to 0.7 s) and a maximum acceleration of 0.5 g.

The experimental determinations yielded the following values for the fundamental natural frequencies:

Table 6 – Fundamental frequencies and stiffness variation determined experimentally

Model	Initial frequency $f_{n,i}$ [Hz]	Initial period $T_i = 1/f_{n,i}$ [s]	Final frequency $f_{n,f}$ [Hz]	Final period $T_f = 1/f_{n,f}$ [s]	Stiffness variation [%]
THS 24-388 (t_otel = 0.84 mm, ρ_EPS = 24 kg/m³)	5.04	0.198	4.63	0.216	−8.1
THS 24-389 (t_otel = 1.09 mm, ρ_EPS = 16.9 kg/m³)	5.70	0.175	4.50	0.217	−19.3

6.2 DAMPING AND NONLINEAR BEHAVIOR

The determination of the fraction of critical damping was performed using both the logarithmic decrement method and the Hilbert envelope analysis applied to the free-vibration response. The results indicate an equivalent damping ratio of:

- **ξ ≈ 1.52 %** in the initial state;
- **ξ ≈ 1.53 %** in the final state, after completion of all tests.

The low value of damping confirms the predominantly elastic behavior of the system, with limited energy dissipation. The main sources of damping were identified as:

- local friction in the contact zones between panels and the lower U-tracks;

- localized deformation around the self-tapping screws;
- partial loss of adhesion between the EPS core and the steel faces.

Although these effects produced a slight local increase in damping, the global behavior remained elastic, without the appearance of plastic dissipation mechanisms such as local buckling or yielding of the steel sheets.

6.3 CORRELATION BETWEEN FORCE AND DISPLACEMENT

The force–displacement curves obtained from the accelerograms and the seismic mass show an almost linear relationship up to Artificial Action 4, followed by a slight nonlinearity during Artificial Action 5 (100 % scaled). The shape of the hysteretic loops is narrow, confirming low energy dissipation and a global response dominated by elasticity.

At the maximum relative displacement of 53 mm—equivalent to a deformation of 1.96 % of the story height (h = 2700 mm)—the structure did not exhibit any loss of stability or major structural degradation.

This behavior confirms that although the displacements exceed the serviceability limit state (SLS) thresholds, they remain below the ultimate limit state (ULS) limit of 2.5 % imposed by code P100-1/2013. Therefore, the system demonstrates good deformation capacity without loss of strength, a favorable characteristic for lightweight prefabricated structures.

6.4 VISUAL OBSERVATIONS AND CORRELATION WITH STRUCTURAL BEHAVIOR

Visual inspections carried out after the last test (Artificial 5 – 0.61 g) revealed slight local deformations of the base U-track and isolated loosening of self-tapping screws. Approximately 1 % of the screws showed partial axial displacement or rotation, and the holes around them became slightly elongated, a phenomenon attributed to cyclic shear demand. The most affected zones were the panel-to-panel joints, where small losses of tightness were observed, without complete detachment or loss of contact.

At the level of the expanded-polystyrene core, a slight local detachment was noticed near the base zone, generated by the alternating tension and compression forces acting on the steel faces. These deteriorations are local and reversible, and the overall appearance of the structure confirms its global integrity and elastic recovery capacity after the seismic actions.

6.5 GENERAL INTERPRETATION

The overall behavior of the tested Thermasteel model is characterized by

- high initial stiffness and good global stability;
- moderate decrease of the natural frequency after successive test series ($\Delta f \approx 20$ %);
- low damping ($\xi < 2$ %), typical of systems with small internal losses;
- relatively large lateral deformability without collapse or loss of continuity;
- local energy-dissipation mechanisms through friction and joint deformation.

In summary, the structure exhibited a safe and controlled seismic response, with limited energy dissipation, predominantly elastic behavior, and the ability to redistribute stresses locally within the connection zones.

7 U.S. SEISMIC COMPLIANCE REFERENCES AND EXPERIMENTAL PERFORMANCE SYNTHESIS

This chapter reproduces the U.S.-style seismic system coefficients and applicability limits referenced in the Thermasteel Load Tables (Table 4 and Section 4.1.1.8) and summarizes peak-based performance indicators measured in the shake-table tests for the tested specimens. The intent is to support transferability discussions for U.S. seismic-zone use by providing both the code-reference context and the measured response.

7.1 U.S. SEISMIC-ZONE COMPLIANCE REFERENCES (THERMASTEEL LOAD TABLES)

Thermasteel's Load Tables provide response modification factor R, overstrength factor Ω_0, and deflection amplification factor Cd, together with maximum permitted building heights by Seismic Design Category (SDC). These values are prescribed by the selected seismic-force-resisting system type.

Table 7.1 *- . Seismic design coefficients and height limits by SDC*

Seismic force-resisting system		Response modification coefficient (R)	Overstrength factor (Ωo)	Deflection amplification (Cd)	Structural system limitations including structural height, hn (ft.) Limits				
					Seismic design category				
					B	C	D	E	F
Bearing wall systems	Light-frame (cold formed steel) walls sheathed with wood structural panels rated for shear resistance or steel sheets	6.5	3	4	NL	NL	65	65	65
	*Light-frame walls with shear panels of all other materials (for example eps)	2	2.5	2	NL	NL	35	NP	NP
	Lift-frame (cold-formed steel) wall systems using flat strap bracing	4	2	3.5	NL	NL	65	65	65
Building frame systems	Light-frame (cold formed steel) walls sheathed with wood structural panels rated for shear resistance or steel sheets	7	2.5	4.5	NL	NL	65	65	65
	*Light-frame walls with shear panels of all other materials (for example eps)	2.5	2.5	2.5	NL	NL	35	NP	NP

Abbreviation used:

- NL = Not Limited
- NP = Not Permitted

*Use **ThermaSteel** shear structural panel with wood or steel sheathings in conjunction with the coefficient, factor, amplification and limitations as allowed by the table for seismic categories **E** and **F**.

Notes:

1. Response modification coefficient, **R**, for use through table. Note that **R** reduces forces to strength level, not an allowable stress level.
2. Where the tabulated value of the overstrength factor **Ωo**, is greater than or equal 2.5, **Ωo** is permitted to be reduced by subtracting the value of 0.5 for structures with flexible diaphragms.
3. An increase in structural height, **hn**, to 45 feet (13.70 meters) is permitted for single-story storage warehouse facilities.

7.2 EXPERIMENTAL PERFORMANCE SYNTHESIS (SHAKE-TABLE TESTS)

This section reports response quantities that are directly measured or derived from measured accelerations and relative displacements. These indicators are commonly used to describe seismic performance (drift demand/capacity and dynamic amplification).

Definitions:

Acceleration amplification factor

$$a_f = \frac{a_{top,peak}}{a_{base,peak}} \tag{7.1}$$

Peak relative acceleration demand

$$\Delta_a = a_{top,peak} - a_{base,peak} \tag{7.2}$$

Peak inertial shear estimate

$$V_{peak} = m \times \Delta_a \times g, g = 9.81\ {}^{m}/_{s^2} \tag{7.3}$$

Peak drift ratio

$$Drift_{peak}(\%) = \frac{\Delta_{rel,peak}}{h} \times 100;\ h = 2705mm \tag{7.4}$$

Peak secant stiffness

$$k_{sec,peak} = \frac{V_{peak}}{\Delta_{rel,peak}} \tag{7.5}$$

Assumption for inertial shear

Unless otherwise stated by the designer, m = 4500 kg is used as participating seismic mass for $m = 4500kg$ is used as participating seismic mass for V_{peak} and $k_{sec,peak}$.

Table 7.2. *Peak-based experimental response indicators*

Model	Test	Record / input motion	$a_{base,peak}$ (g)	$a_{top,peak}$ (g)	a_f	Δ_a (g)	$\Delta_{rel,peak}$ (mm)	Drift, peak (%)	V_{peak} (kN)	$k_{sec,peak}$ (kN/mm)
THS 24-388	20	R5 – Artificial Ar02	0.380	0.920	2.421	0.540	8	0.296	23.838	2.980
THS 24-388	30	R15 – Turkey 2023 modified	0.500	1.210	2.420	0.710	11	0.407	31.343	2.849
THS 24-388	37	R22 – Vrancea 1977 modified	0.250	0.630	2.520	0.380	12	0.444	16.775	1.398
THS 24-388	40	R30 – Turkey 2023 modified	0.350	1.040	2.971	0.690	13	0.481	30.460	2.343
THS 24-388	46	R36 – Artificial Ar02	0.410	1.050	2.561	0.640	18	0.665	28.253	1.570
THS 24-389	40	Vrancea 1977 scaled 130%	0.260	0.490	1.885	0.230	7	0.259	10.153	1.450
THS 24-389	41	Northridge 1994 scaled 100%	0.390	0.920	2.359	0.530	26	0.961	23.397	0.900
THS 24-389	43	Turkey 2023 modified 80%	0.430	1.230	2.860	0.800	28	1.035	35.316	1.261
THS 24-389	48	Artificial 5 scaled 80%	0.440	1.280	2.909	0.840	30	1.109	37.082	1.236
THS 24-389	49	Artificial 5 scaled 100%	0.610	1.450	2.377	0.840	53	1.959	37.082	0.700

7.3 MAPPING STATEMENT FOR U.S. TRANSFERABILITY

For U.S. seismic-zone compliance, the designer must select the applicable seismic-force-resisting system type from Table 7.1 based on the as-built configuration. The tested specimens provide experimental evidence of drift demand, acceleration amplification, and global stability, but they do not, by themselves, assign or certify the code coefficients R, Ω_0, and Cd. Those coefficients remain code-prescribed by system type.

Based on the as-built bracing and hold-down detailing, the ThermaSteel panel system shall be classified by the Engineer of Record as one of the seismic-force-resisting systems listed in ThermaSteel Load Tables. The corresponding code coefficients (R, Ω_0, Cd) and SDC height limitations apply. The shake-table tests reported here provide supporting performance data (peak drift ratios and dynamic amplification) for the tested configuration.

7.4 LIMITATIONS

1. The inertial shear V_{peak} is an estimate based on measured accelerations and an assumed participating mass; it is intended for performance reporting, not for direct design without an explicit mass definition.
2. This annex does not replace code-required analyses (ASCE 7 / IBC) or required qualification procedures.
3. System classification and detailing requirements (e.g., hold-down/track design) remain the responsibility of the Engineer of Record.

8 CONCLUSIONS

The experimental program carried out on the ThermaSteel structural models THS 24-388 and THS 24-389 aimed to evaluate the dynamic behavior and the seismic energy dissipation capacity of a single-story structural system made of sandwich panels with cold-formed thin steel profiles and an expanded polystyrene (EPS) insulating core. The results obtained from the seismic platform tests showed a globally stable behavior, without instability phenomena or loss of structural continuity.

From the analysis of the free vibration tests, the initial and final fundamental frequencies were determined. For THS 24-388, the frequency decreased from 5.04 Hz (T = 0.198 s) to 4.63 Hz (T = 0.216 s), and for THS 24-389, from 5.70 Hz (T = 0.175 s) to 4.50 Hz (T = 0.22 s). This reduction of 8–20% indicates a moderate decrease in dynamic stiffness, associated with small local nonlinearities at the joints and at the panel-to-floor connections, without affecting the overall structural stability. The final values of the fundamental periods, ranging between 0.17 and 0.22 s, are characteristic of lightweight structures with low mass and high stiffness.

The equivalent damping ratio determined experimentally ranged between ξ = 1.52–1.53%, both before and after the seismic tests. These low damping values confirm the predominantly elastic behavior typical of lightweight systems, where energy dissipation occurs mainly through internal friction in joints and local deformation of the steel sheet around the screws. No significant plastic mechanisms or global loss of adhesion between the steel faces and the insulating core were observed.

During the most severe excitation (Artificial 5 – 100% scaled, maximum acceleration 0.61 g), the maximum relative displacement measured between the floor slab and the top of the structure was 53 mm, corresponding to a drift of 1.96% of the story height (h = 2700 mm). According to P100-1/2013, this value exceeds the serviceability limit state (SLS) but remains below the ultimate limit state (ULS) of 2.5%·h, confirming the structural safety and stable performance of the system under strong seismic actions.

Visual inspections performed after the final tests revealed only local damage: isolated (approximately 1%) loosening of self-tapping screws, slight deformations in the base U-track, and partial loss of adhesion between the EPS core and the steel faces, limited to the lower areas of the panels. These phenomena are localized and reversible, without affecting the load-bearing capacity or global stiffness of the structure.

In comparison, model THS 24-389 (steel faces 1.09 mm thick, EPS density 16.9 kg/m^3) exhibited higher stiffness, smaller displacements, and tighter behavior at the joints than model THS 24-388 (steel 0.84 mm, EPS 24 kg/m^3). Increasing the thickness of the steel profiles has a dominant influence on bending stiffness and lateral displacement control, while the density of the EPS core plays a secondary role. Conversely, the structure with thinner steel faces and denser core showed slightly higher damping, caused by internal friction and local deformations around the screws.

Overall, the ThermaSteel system demonstrated a global elastic, stable, and predictable behavior, with good deformation capacity and nearly complete recovery to the initial position after the cessation of seismic motion. Although small nonlinearities were observed in the joint zones, the structure showed no signs of instability and continued to act as a unified structural system. The results confirm the reliability of the Thermasteel system for single-story lightweight buildings in seismic regions, where an optimal balance between low weight, sufficient stiffness, and safe dynamic performance is required.

9 ANNEXES

In addition to this report, an archive has been provided containing the raw data files for the recorded accelerations and displacements from the performed tests, as well as the corresponding video recordings.

- Accelerations: CSV files containing raw acceleration records.
- Displacements: CSV files containing raw displacement records.
- Video: Model **THS 24-388** https://youtu.be/gNKNPZ7_pco
- Video: Model **THS 24-389** https://youtu.be/XDudUWT1-5g